Crystallization of Gas-Laden Amorphous Water Ice, Activated by Heat Transport to its Subsurface Reservoirs, as Trigger of Huge Explosions of Comet 17P/Holmes

Zdenek Sekanina

Jet Propulsion Laboratory; California Institute of Technology; Pasadena, CA 91109; U.S.A.

Abstract. *Thick terrain layers, of the type recognized on the* Deep Impact *mission's close-up images of the nucleus of comet 9P/Tempel, and each 10^{13} to 10^{14} grams in mass, are suggested to be attractive candidate carriers of solid material released into the atmosphere during super-massive explosions (megabursts) and/or major fragmentation events. The properties of the 2007 megaburst of comet 17P/Holmes are shown to be consistent with the triggering mechanism being a transformation of gas-laden water ice from low-density amorphous phase to cubic phase (crystallization) in a reservoir located beneath a layer tens of meters thick. Molecules of highly volatile gases, carbon monoxide in particular, trapped in amorphous water ice and released during the phase transition (at 130 °K to 150 °K), are superheated, generating — almost instantly in a runaway process — a momentum needed to lift off, from the comet's nucleus, the mass of the layer and, after its collapse, to accelerate the pile of mostly microscopic dust debris to subkilometer-per-second velocities. Strongly temperature dependent, the crystallization rate increases progressively between ~ 100 °K at aphelion and nearly 120 °K (with ~ 10 percent of the ice in cubic phase) some 10 days before the megaburst and explosively afterwards, due to the release of the trapped volatiles and completion of the phase transition. The proposed model is in agreement with a wide range of relevant observations of the 2007 megaburst of comet 17P, including the event's post-perihelion timing, the water production rate, the CO-to-H_2O production rate ratio, the dust halo's expansion rate, and the energy involved. The observed recurrence rate of super-massive explosions of comet 17P is explained by heat transport through the terrain layers whose effective thermal conductivity is about 0.2 W m^{-1} $°K^{-1}$.*

1. Introduction

In October 2007, comet 17P/Holmes underwent a super-massive explosion (megaburst), during which it brightened almost a million times in about 2 days. Its intrinsic magnitude (normalized to unit geocentric and heliocentric distances by an inverse-square power law) reached −0.5 (Sekanina 2009a) to become comparable to the intrinsic magnitude of some of the brightest comets ever observed, such as the sungrazer C/1882 R1. The mass of a cloud of microscopic dust suddenly injected into the atmosphere of 17P/Holmes during the megaburst was estimated at 10^{14} g (Sekanina 2008a, hereafter referred to as Paper 1; and confirmed independently by Schleicher 2009), exceeding by orders of magnitude the amounts of dust released in conventional outbursts originating from relatively small, isolated emission centers on the nuclear surface of many comets. Because of the enormous rate of dust injection into the comet's atmosphere, I argued in Paper 1 that the megaburst must have been an event of global proportions on the scale of the comet's nucleus, involving a surface unit of considerable areal extent (several km^2) and substantial thickness (tens of meters), and that the injected mass must have collapsed upon liftoff into a pile of predominantly microscopic debris. This scenario requires major sources of volatile material stored in the comet's interior and a sufficiently powerful trigger mechanism not only for the liftoff, but also for the acceleration of a significant fraction of particulate ejecta to explain the observed expansion, at a rate of 0.50 km/s, of the disk-shaped, sharply-bounded dust halo observable for days, weeks, or even months after the event's termination.

The 2007 megaburst of 17P/Holmes was not this comet's first major explosion. The object was in fact discovered while flaring up in early November 1892 (Holmes 1892) and a second, undoubtedly related explosive episode was detected some 10 weeks later, in early 1893 (Palisa 1893). No additional explosion of a similar magnitude is known to have occurred between 1892-1893 and 2007,[1] and one can essentially rule out that another such event was missed during the intervening period of time (Sekanina 2009b, hereafter referred to as Paper 2). From the available data (*e.g.*, Bobrovnikoff

[1] From a recent analysis of the light curves of 17P/Holmes, Sekanina (2009a) concluded that a moderate outburst occurred in June 1899, ~ 70 days after perihelion. Possibly related to the 1892-1893 episodes, it produced no dust halo and is not classified as a super-massive explosion.

1943), it appears that the two episodes of the 19th century super-massive explosion were not as powerful as the 2007 megaburst, their combined dust-mass loss estimated in Paper 1 at about 30 percent of the mass lost in 2007.

While the 2007 megaburst of 17P/Holmes remains unrivaled as the most powerful event of this kind on record, it is now known that comet 1P/Halley underwent a major explosion $\sim$ 10 weeks after its 1835 perihelion passage (Sekanina 2008b), an event that probably was more powerful than 17P/Holmes' 1892-1893 episodes. It is likely that super-massive explosions are more common than they appear to be, and because 17P and 1P have different histories, the process is not restricted to a particular category of comets.

I concluded in Paper 2 that there is no evidence for super-massive explosions of comet 17P to recur on a time scale shorter than 16 revolutions about the Sun, which is currently about 115 years. Even though this result, of major importance for understanding the role of these events in the long-term evolution of comet 17P, lacks a statistical significance, it is in fair agreement with an estimate of 0.01 per year per comet for a minimum rate of cometary splitting (Chen and Jewitt 1994), an apparently related process (Secs. 2 and 3).

2. Terrain Layering on Comets of Jupiter Family, and Cometary Fragmentation

A major discovery reported from the *Deep Impact* close-up imaging of comet 9P/Tempel (Thomas *et al.* 2007) was an extensive stratigraphic arrangement of its surface into pervasive, mostly inert layers tens to 200 meters thick, each extending up to several km^2 on the nucleus surface and subjected to gradual erosion.

Belton *et al.* (2007) regarded the layers to be (a) a relict of a primordial process involving porous aggregate bodies in the early agglomeration phase and (b) ubiquitous on the nuclei of Jupiter family comets (cf. also Sec. 10). In this model, the nuclear interior consists of a core overlain by a pile of randomly stacked layers, each estimated to have typically a base area of $\sim$ 5 km^2, a thickness of $\sim$ 50 meters, and a mass of $\sim 10^{14}$ g at a bulk density of 0.4 g cm^{-3}. The remarkable match between the typical mass of a thick layer and the mass of particulates in the post-megaburst halo of 17P/Holmes makes such layers *attractive candidate carriers* of dust released in super-massive explosions.

The potential role of thick layers as a feed for super-massive explosions parallels my earlier finding (Sekanina 1982) that companion nuclei of split comets must be strongly flattened or *pancake shaped*, in order to explain a mismatch between their observed brightness and the outgassing-driven differential nongravitational deceleration in their motions relative to the principal nucleus. The dimensions inferred for major, most-persistent companions suggest masses of $\sim 10^{14}$ g (Paper 1), again on a par with the masses of thick layers and 17P/Holmes' dust halo. Comets of all categories, of the Jupiter family and nearly parabolic orbits alike, are known to experience splitting.

The smooth terrains, a subcategory of the layering topography on the surface of comet 9P/Tempel, may be a result of a recent — and perhaps still ongoing — process. Various mechanisms, including cryogenic volcanism and activity similar to the formation of terrestrial pyroclastic flows, have been suggested by different research groups and summarized and discussed by Belton and Mellish (2009). Most of these phenomena occur on scales that are generally much smaller than the super-massive explosions, but the extent of the largest flow fields on comet 9P have been estimated by Belton and Mellish at $\sim$ 2 km^2.

3. The Energy Source and Triggering Mechanism

A general objective of this investigation is to contribute to the understanding of a potential role of thick, extended, mostly inert terrain layers — regardless of their history, age, and origin — in the evolution of the cometary nuclei with this stratified structure. A specific goal is to examine in detail a physical process on the surface and in the interior of comets that results in a super-massive explosion of comet 17P/Holmes in particular and, by inference, in nuclear fragmentation in general. As described in Paper 1, the suggested process for comet 17P — of global proportions on the scale of its nucleus — is a continual removal of stacked terrain layers, one by one, over long periods of time. This conceptual scenario implies that super-massive explosions are recurring events in which the jettisoned mass, of excessively low mechanical strength, suddenly collapses into a pile of mostly microscopic dust upon the liftoff (Sec. 1). Splitting and super-massive explosions are therefore indeed two manifestations of the same process, a conclusion that is supported by Stevenson *et al.*'s (2009) observations of 16 transient minifragments in comet 17P. If a major part of the layer survived the liftoff either intact or broken into only a few sizable fragments, an event of full-scale splitting would have resulted instead of a megaburst, with most mass concentrated in the slowly receding companion nucleus (or nuclei) rather than in the rapidly expanding halo.

In the proposed scenario, each terrain layer's liftoff from the surface of the nucleus is driven by water vapor expanding from the proposed reservoir of ice situated beneath each such layer, following an exothermic reaction accompanying a transition of water ice from low-density amorphous phase to cubic phase. With a sudden release of energy of 100 J g^{-1} (Ghormley 1968), the ice gets heated up by tens of degrees K, increasing the vapor pressure by orders of magnitude. This scenario was considered in Paper 1 as tentative, subject to support from detailed heat-diffusion calculations, which are presented in this paper.

As a potential trigger for cometary outbursts, the exothermic reaction driven by the amorphous-to-cubic water ice phase transition was first proposed by Patashnick *et al.* (1974). They showed that the crystallization mechanism is appropriate for outbursts of usual intensity, with the total mass of released material of about 10^{12} g or less. More recently, the role of crystallization of water ice and the stratified structure of cometary nuclei have been considered on a number of occasions and summarized by Prialnik *et al.* (2004) in their review of modeling the activity of comets. Although some of Patashnick *et al.*'s input numbers are outdated, the main difference between their outbursts and the super-massive explosions like the 2007 megaburst of comet 17P/Holmes is that the latter involve dust ejecta that are

orders of magnitude greater in mass.

Assuming the existence of a reservoir of amorphous water ice beneath each thick layer, two critical problems need to be resolved: (i) whether heat transport into a comet's interior can lead to an *in situ* explosive amorphous-to-cubic phase transition of water ice, and (ii) whether the energy released by the exothermic reaction is capable of generating a momentum required to lift off a layer of 10^{14} g resting on top of the ice reservoir.

4. Condition for Lifting Off a Terrain Layer

The second problem can be addressed by comparing the gravitational force $F_{\rm grav}$ of the nucleus on the layer with the drag force $F_{\rm drag}$ that the molecules sublimating from the ice reservoir exert in the direction opposite to gravity. Using a notation similar to that applied by Delsemme and Miller (1971) to the case of dust-particle ejection, the gravitational force on the surface of the nucleus, whose diameter is D and bulk density ρ, is

$$F_{\rm grav} = \frac{2}{3}\pi G D \rho A_{\rm layer} \eta_{\rm layer} \rho_{\rm layer}, \tag{1}$$

where G is the gravitation constant and $A_{\rm layer}$, $\eta_{\rm layer}$, and $\rho_{\rm layer}$ are, respectively, the base area, the thickness, and the bulk density of the layer. The molecular drag force is

$$F_{\rm drag} = 2 m v_0(T_{\rm cryst}) Z(T_{\rm cryst}) A_{\rm layer}, \tag{2}$$

where m is the mass of a water molecule, $T_{\rm cryst}$ is the temperature to which the ice is heated up by the exothermic reaction, $v_0(T_{\rm cryst})$ and $Z(T_{\rm cryst})$ are, respectively, the mean molecular velocity in the direction away from the nucleus and the H_2O outgassing flux per unit area, and $2mv_0(T_{\rm cryst})$ is the momentum exerted on the layer's flat base area. The layer is lifted from the surface of the comet when $F_{\rm grav} < F_{\rm drag}$, or its thickness

$$\eta_{\rm layer} < \frac{3 m v_0(T_{\rm cryst}) Z(T_{\rm cryst})}{\pi G D \rho \rho_{\rm layer}}. \tag{3}$$

As expected, the condition is independent of $A_{\rm layer}$ when the ice reservoir extends beneath the entire base area of the layer. For comet 17P/Holmes, I use $D = 3.3$ km (Lamy *et al.* 2000; Snodgrass *et al.* 2006) and $\rho = 0.4$ g cm^{-3} (Richardson *et al.* 2007), and assume $\rho_{\rm layer} \simeq \rho$ and, for water vapor, $v_0 \simeq 0.5$ km/s. With the standard values for G and m, one finds that to lift off a 50-meter-thick layer requires at least $Z \simeq 1.2 \times 10^{19}$ mol cm^{-2} s^{-1} or 31 g cm^{-2} day^{-1}, corresponding to $T_{\rm cryst} \simeq 220$°K. Thinner layers can be lifted off at lower temperatures.

5. Exothermic Process of Crystallization

Different critical temperatures, from less than 140°K up to $\sim$ 160°K, are quoted in the literature for the transition of water ice from amorphous phase to cubic phase. This is so because the crystallization process takes place in a broad range of temperatures at strongly temperature-dependent rates, as established experimentally by Schmitt *et al.* (1989). They measured the crystallization rates of pure water ice and its mixtures with carbon monoxide and carbon dioxide at a number of temperatures ranging from 125°K to 150°K. By monitoring changes in the infrared absorption bands of H_2O, they were able to determine the time needed to complete the transition of pure water ice from amorphous to cubic phase as a function of temperature T. The crystallization rate $\Re_*(T)$ (in s^{-1}), given as a reciprocal of the crystallization time $t_*(T)$, varies according to Schmitt *et al.* (1989) exponentially with $1/T$ (in °K),

$$\Re_*(T) = \frac{1}{t_*(T)} = 1.05 \times 10^{13} \exp\left(-\frac{5370}{T}\right). \tag{4}$$

Extrapolation of this law suggests that ice crystallization occurs instantly (in seconds) at 170°K, while it takes several hundred years near 100°K and is comparable with the age of the solar system just below 80°K. A transition from high-density to low-density amorphous ice occurs between 38°K and 68°K (Jenniskens and Blake 1994, 1996).

The strong temperature dependence of the crystallization rate indicates that, over a number of revolutions about the sun, the process in comets steadily accelerates with time along the interface between the layer and the ice reservoir. The outgassing rate from the ice increases progressively with time in both amorphous and cubic phases (pre- and post-transition), due to heating from the exothermic reaction. This is a typical case of a self-feeding mechanism, as pointed out by Patashnick *et al.* (1974). Temperature dependent values of the specific heat of water ice, $C_{\rm ice}$, available from textbooks on its thermal properties, can closely be approximated by an expression

$$C_{\rm ice}(T) = (c_1 - c_2 T) T, \tag{5}$$

where $c_1 = 8.68 \times 10^4$ erg g^{-1} °K^{-2} and $c_2 = 37.7$ erg g^{-1} °K^{-3}. $C_{\rm ice}$ is in the units of erg g^{-1} °K^{-1}. Equating the heat of crystallization $E_{\rm cryst} = 10^9$ erg g^{-1} (Ghormley 1968), supplied by the exothermic reaction, with the energy needed to heat ice up from an initial temperature $T_{\rm init}$ to a final temperature $T_{\rm fin}$,

$$E_{\rm cryst} = \int_{T_{\rm init}}^{T_{\rm fin}} C_{\rm ice}(T) dT = \frac{1}{2} c_1 \left(T_{\rm fin}^2 - T_{\rm init}^2\right) - \frac{1}{3} c_2 \left(T_{\rm fin}^3 - T_{\rm init}^3\right), \tag{6}$$

one can solve the resulting cubic equation for $T_{\rm fin}$ iteratively from the following expression:

$$T_{\rm fin} = \sqrt{T_{\rm init}^2 + \frac{2.30 \times 10^4}{1 - 2.90 \times 10^{-4} \frac{T_{\rm fin}^3 - T_{\rm init}^3}{T_{\rm fin}^2 - T_{\rm init}^2}}}. \tag{7}$$

Starting with $T_{\rm fin} = T_{\rm init}$ under the square-root sign, when the fraction in the denominator is reduced to $\frac{3}{2}T_{\rm init}$, this iteration converges rapidly.

6. Crystallization of Pure Water Ice

One can only speculate about the physical conditions in the putative ice reservoir beneath the terrain layer in the course of the phase transition. Water ice is assumed to dominate, but it is most likely to be mixed with dust and contaminated by other, more-volatile ices (Sec. 7). The scenarios examined in this section are based on pure amorphous ice of water. Although other sources and sinks of energy may be involved, I consider only the role of the heat of crystallization released during the transition of amorphous ice to cubic ice. Because a fraction of the sun's energy incident on the surface of the nucleus (*i.e.*, on the outer boundary of the essentially inert layer) is conducted into the comet's interior, the temperature at the interface between the layer's base and the reservoir must steadily increase over long periods of time because of heat transport, an issue that is addressed in Sec. 9.

Although not strictly defined, the temperature $T_{\rm init}$, the basic parameter for tracking the evolution of crystallization effects, must for comet 17P/Holmes be chosen in such a manner that the resulting *nominal* scenario conforms to a rule-of-thumb constraint that the crystallization time at $T_{\rm init}$ be much longer than 115 years, the time span between the comet's 1892-1893 and 2007 explosions. However, $T_{\rm init}$ should not be chosen too low, because the rates of cubic-ice formation under such physical conditions become trivial and can be neglected. Also, the final temperature $T_{\rm fin}$ from such solutions would differ very little from that in the nominal scenario, whereas accounting for a long-term temperature increase at the layer's base due to heat transport (Sec. 9) would complicate the numerical approach.

Next, I introduce a characteristic time $t_{\rm ice}$, which measures the duration of the crystallization process by integrating the crystallization time t_* from an initial temperature $T_{\rm init}$ to a final temperature $T_{\rm fin}$,

$$t_{\rm ice}(T_{\rm init}, T_{\rm fin}) = \frac{1}{E_{\rm cryst}} \int_{T_{\rm init}}^{T_{\rm fin}} t_*(T) C_{\rm ice}(T) {\rm d}T. \tag{8}$$

Because the early phase of the crystallization process contributes very little to the integrated effect, a realistic characteristic time should be on the order of the orbital period. Inserting the expressions from Equations (4) and (5), the characteristic time (in s) is, after integrating Eq. (8), equal to

$$t_{\rm ice}(T_{\rm init}, T_{\rm fin}) = \alpha \left[{\rm Ei}\left(\frac{5370}{T_{\rm init}}\right) - {\rm Ei}\left(\frac{5370}{T_{\rm fin}}\right) + \Psi(T_{\rm init}) - \Psi(T_{\rm fin}) \right], \tag{9}$$

where $\alpha = 2.657 \times 10^{-11}$ s, ${\rm Ei}(x)$ is the exponential-integral function, and

$$\Psi(x) = \left(\frac{x}{2808.93}\right)^3 \exp\left(\frac{5370}{x}\right) \left[1 - \frac{768.58}{x} - \left(\frac{2031.58}{x}\right)^2 \right]. \tag{10}$$

The exponential-integral function can be calculated using Euler's constant **C** and a series,

$${\rm Ei}(x) = \mathbf{C} + \ln x + \sum_{k=1}^{\infty} \frac{x^k}{k \cdot k!}, \tag{11}$$

with up to 100-150 terms that warrant formal precision to about ten decimals.[2]

Table 1 lists, as a function of an initial temperature $T_{\rm init}$, the final temperature $T_{\rm fin}$ derived from Eq. (7), the temperature increase $\Delta T_{\rm fin} = T_{\rm fin} - T_{\rm init}$, the crystallization time $t_*(T_{\rm init})$ from Eq. (4), and the characteristic time $t_{\rm ice}(T_{\rm init}, T_{\rm fin})$ from Eq. (9). The crystallization time equals 115 years at $T_{\rm init} = 103.^\circ3$ K, while $T_{\rm fin} = T_{\rm cryst} = 220^\circ$K, needed for lifting off a terrain layer (Sec. 4), when $T_{\rm init} = 152.^\circ6$ K. From the two constraints, on t_* and $t_{\rm ice}$, an estimated initial temperature for the crystallization process in a reservoir of pure water ice is consistently confined to a narrow range, $T_{\rm init} = 100^\circ$K to 102°K, the corresponding final temperature $T_{\rm fin}$ being near 187°K, more than 30°K below the critical temperature $T_{\rm cryst}$ of 220°K, required by condition (3). The conclusion is that the *phase transition from amorphous to cubic phase in a reservoir of pure water ice does not generate enough momentum to lift off terrain layers ~ 50 meters thick from the nuclear surface to the atmosphere.*

Rather than readily conceding this verdict, I first verify the time scale of the crystallization process and temporal variations in the rate of cubic-ice formation by a direct, step-by-step approach, in which $E_{\rm cryst}$ is, as before, the energy released per gram of transformed ice and the initial conditions, at time t_0, include a mass $\mathcal{M}_0$ of amorphous ice and its

[2] High-precision values of the exponential-integral function ${\rm Ei}(x)$ can be obtained from various web sites, such as `http://keisan.casio.com`.

Table 1. Pure water ice temperature jump and the crystallization and characteristic times.

Water ice temperature			Crystallization time, $t_*(T_{\rm init})$	Characteristic time, $t_{\rm ice}(T_{\rm init}, T_{\rm fin})$
$T_{\rm init}$ (K)	$T_{\rm fin}$ (K)	$\Delta T_{\rm fin}$ (K)		
98.0	185.0	87.0	1900 yr	28.8 yr
99.0	185.5	86.5	1090 yr	17.1 yr
100.0	186.1	86.1	634 yr	10.2 yr
101.0	186.6	85.6	372 yr	6.20 yr
102.0	187.2	85.2	221 yr	3.79 yr
103.3	187.9	84.6	***115 yr***	2.05 yr
104.0	188.3	84.3	80.4 yr	1.46 yr
106.0	189.5	83.5	30.3 yr	214 d
108.0	190.7	82.7	11.9 yr	88.5 d
110.0	191.8	81.8	4.81 yr	37.9 d
115.0	194.9	79.9	210 d	5.19 d
120.0	198.0	78.0	30.0 d	20.3 hr
130.0	204.4	74.4	23.1 hr	49.6 min
140.0	211.1	71.1	1.21 hr	3.25 min
150.0	218.1	68.1	5.61 min	18.6 s
152.6	***220.0***	67.4	3.05 min	10.7 s
160.0	225.3	65.3	35.9 s	2.42 s

◇ ◇ ◇

(text continued from page 102)

temperature $T_0 = T_{\rm init}$. To keep this exercise straightforward, no dust contamination has been considered. At time $t > t_0$, when the remaining mass of amorphous ice is $\mathcal{M}(t)$ and its temperature is $T(t)$, the crystallization process continues at a rate $\Re_*(T)$ given by Eq. (4). During a very short interval of time Δt, whose length is allowed to vary with time, the mass of cubic ice formed between t and $t + \Delta t$ is $\mathcal{M}(t)\ \Re_*(T)\ \Delta t$. The mass of remaining amorphous ice is, at time $t + \Delta t$, equal to $\mathcal{M}(t)[1 - \Re_*(T)\Delta t]$. The energy $\mathcal{M}(t)\ \Re_*(T)\ E_{\rm cryst}\ \Delta t$ provided by crystallization between t and $t + \Delta t$ is used to increase the temperature of all ice from T at time t to $T + \Delta T$ at $t + \Delta t$:

$$\Delta T = \frac{\mathcal{M}(t)\Re_*(T)E_{\rm cryst}\Delta t}{\mathcal{M}_0 C_{\rm ice}(T)}. \tag{12}$$

From extremely low saturated pressures in the temperature range under consideration, it follows that both the mass of water vapor and its sublimation energy contribute negligibly to the balance.

After k steps, the total energy spent on increasing the temperature in the ice reservoir is

$$\mathcal{M}_0 \sum_{i=1}^{k} C_{\rm ice}(T)\Delta T \le \mathcal{M}_0 E_{\rm cryst} \tag{13}$$

and the mass of remaining amorphous ice is

$$\mathcal{M}(t_k) = \mathcal{M}_0 \prod_{i=1}^{k} [1 - \Re_*(T)\Delta t] < \mathcal{M}_0. \tag{14}$$

The goal of this exercise is to find, via the number of steps n, the corresponding time t_n by which all released energy had been spent and the crystallization process terminated. The difference between t_0 and t_n is a finite period of time, $t_{\rm cubic}$, which should be identical with the characteristic time,

$$t_{\rm cubic} = t_n - t_0 = \sum_{i=1}^{n} \Delta t = t_{\rm ice}. \tag{15}$$

It is noted that, with the equal sign, Eq. (13) converges to Eq. (6) and that the results are independent of $\mathcal{M}_0$, thus:

$$\lim_{\Delta T \to 0} \sum_{i=1}^{n} C_{\rm ice}(T)\Delta T = \int_{T_{\rm init}}^{T_{\rm fin}} C_{\rm ice}(T)\mathrm{d}T = E_{\rm cryst} \tag{16}$$

and

$$\lim_{\Delta t \to 0} \prod_{i=1}^{n} [1 - \Re_*(T)\Delta t] = 0. \tag{17}$$

Because of the exponential increase in the rate $\Re_*(T)$ with time, the convergence takes place at a finite value of n, as also shown by Eq. (15). In particular, Eq. (17) can be zero only when the last multiplier is zero, which requires that

$$\Re_*(T_{\rm fin}) = \frac{1}{t_*(T_{\rm fin})} = \frac{1}{\Delta t}. \tag{18}$$

For example, $\Re_* \simeq 5\ {\rm s}^{-1}$ for $T_{\rm fin} \simeq 190$°K, so that the maximum acceptable step is then about 0.2 s. In actual calculations, a highly variable step has been used, from about 0.5 day near aphelion down to values orders of magnitude smaller than 0.2 s near the end of the numerical scheme, which resulted in $T_{\rm fin}$ agreeing formally with its value from Eq. (7) to better than 0°.01 K.

The step-by-step approach has confirmed the conclusion based on Eqs. (6) and (9) that, in general, terrain layers some 50 meters thick could not be lifted from the surface of comets like 17P/Holmes by a momentum generated as a result of crystallization of pure water ice stored in subsurface reservoirs and that, in particular, this process fails to explain 17P/Holmes' 2007 megaburst or similar super-massive explosions.

7. Crystallization of CO-Laden Water Ice

I now turn to a mechanism that includes more volatile species. The process of water-ice crystallization is retained as a trigger mechanism, but also involved is activation of a gas or gases, such as carbon monoxide, trapped initially in amorphous ice over long periods of time at low temperatures and released suddenly in large quantities during the water-ice phase change. I show below that *it is this release of trapped volatile gases that is the driver of the explosive event itself*, providing a range of different, but rather similar, scenarios.

Besides pure water ice, Schmitt *et al.* (1989) investigated the crystallization process for amorphous water ice mixed with several volatile species, including carbon monoxide and carbon dioxide. For CO, which for its high volatility is of particular interest, they began with a 22-percent CO/H_2O abundance ratio at 10°K and found that by the time the temperature reached 70°K, the abundance ratio dropped to 11 percent, leveling off between 70°K and 130°K. This is apparently the maximum amount of CO that amorphous ice can trap at these higher temperatures. Nearly complete depletion of CO in Schmitt *et al.*'s experiments occurred between 130° and 140°K.

The crystallization rate $\Re_\star(T)$ and time $t_\star(T)$ of CO-laden water ice depend on the temperature in a manner similar to that for pure ice, except that the slope is steeper and the process is slowed down. Schmitt *et al.*'s (1989) graphical fit to the crystallization time corresponds to a rate

$$\Re_\star(T) = \frac{1}{t_\star(T)} = 2.56 \times 10^{14} \exp\left(-\frac{5940}{T}\right), \tag{19}$$

where $\Re_\star$ is again in ${\rm s}^{-1}$ and T in °K.

Schmitt *et al.*'s (1989) result that CO depletion occurs at temperatures 130°K to 140°K agrees with the findings by Bar-Nun *et al.* (1985), whose laboratory experiments indicated a sharply-peaked rate of released CO, CH_4, Ar, and N_2 in a temperature range of 135° and 155°K on small samples, and by Bar-Nun and Laufer (2003), who confirmed bursts of released Ar on large samples between 140°K and 150°K. They invoked the same mechanism as Schmitt *et al.*, calling it dynamic percolation (Laufer *et al.* 1987). Besides the huge spike of released gas, Bar-Nun and Laufer (2003) also detected a slightly delayed and less prominent peak in the pressure (production) of water (see their Figure 1). As CO sublimates profusely already at temperatures of 30°K to 60°K, its molecules released at 130°K to 150°K are superheated, probably transferring some of their energy to the ambient water ice (Sec. 8).

The step-by-step procedure of Sec. 6 can be applied to CO-laden water ice, if the rate of cubic-ice formation $\Re_*(T)$ and the crystallization time $t_*(T)$ for pure water ice are replaced, respectively, with the rate $\Re_\star(T)$ and the crystallization time $t_\star(T)$ from Eq. (19). In what is referred to as a nominal scenario, the crystallization process in CO-laden amorphous ice is assumed to have begun when comet 17P/Holmes passed through aphelion for the last time before the megaburst. From the event's known onset time, 172.2 days after perihelion (Sekanina 2009a), and the 2007 osculation orbital period, 6.886 years or 2515 days, it follows that the megaburst began 1430 days, or 0.57 revolution about the sun, after the comet's passage through aphelion. To transform all CO-laden amorphous ice to cubic ice during the 1430 days, the nominal scenario requires an initial temperature $T_{\rm init} = 106°.37$ K.

The ice-temperature variations due to crystallization are, as a function of time, presented in Figure 1. The rate of temperature increase is seen to be very gradual during most of the time, as a small fraction of amorphous ice, not exceeding a few percent, is being transformed to cubic ice. At only about 10 days before the explosion, when the fraction of cubic ice tops 10 percent, the rate of temperature rise begins to accelerate rapidly. When the spike of released CO sets in, at $\sim$ 130°K, nearly $\frac{1}{4}$ of all ice has been transformed to cubic phase and the temperature now increases precipitously. This is the onset of the megaburst. Its termination at a time by which practically all trapped CO has been released at $\sim$ 150°K occurs 0.10 day later, so this is the duration of the event. All amorphous ice has been transformed to cubic

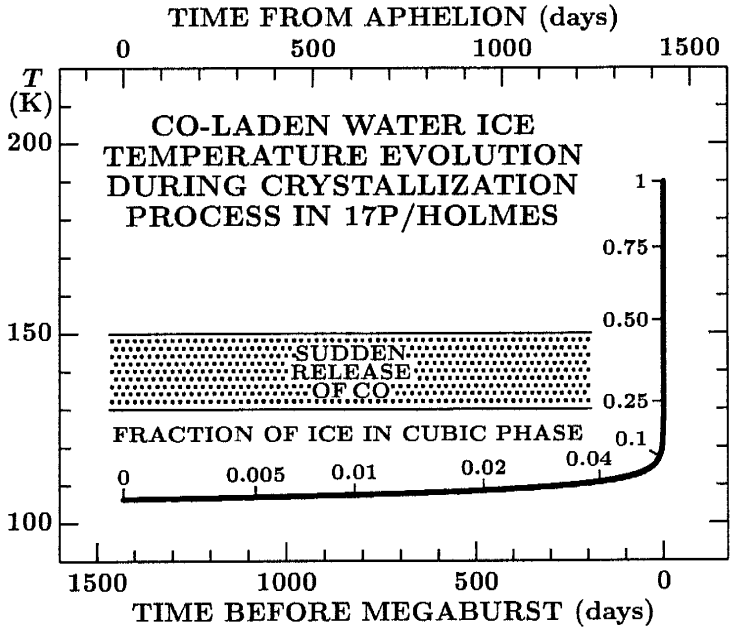

Figure 1. A plot of temperature evolution of CO-laden water ice with time from the aphelion to the megaburst. The temperature's sharp upswing starts at ~ 117° K, some 10 days before the megaburst, when the fraction of ice in cubic phase is about 10 percent. The explosive nature of the final stage of this process, during which all CO is released, is described by the predicted durations of 0.1 day needed to raise the temperature from 130° K to 190° K and only ~ 30 seconds from 150° K to 190° K.

◇ ◇ ◇

(text continued from page 102)

phase by the time the temperature reaches 189°.7 K, only ~ 30 seconds later. An average rate of temperature increase during this brief interval of time is 1°.3 K/s.

The stated lack of sensitivity to the choice of the initial time and temperature can be tested by comparing the nominal scenario, covering a period of 0.57 revolution about the sun and ending with the 2007 megaburst, with an extended scenario that involves a much longer interval of time that also ends with the 2007 megaburst but begins at the aphelion of 1895, which followed the 1892 apparition with the two explosive episodes. The average orbital period of comet 17P/Holmes between 1892 and 2007 was 2622.6 days or 7.180 years. The time from the 1895 aphelion to the 2007 megaburst spans more than 40800 days or 15.57 revolutions. In order to transform all amorphous ice to cubic ice in this period of time, the initial temperature must have been $T_{\rm init}$ = 100°.03 K. The evolution of the water-ice temperature and the fraction of ice in cubic phase are summarized in Table 2, which shows that during the 15 revolutions about the sun, measured from aphelion to aphelion, only about 5 percent of all amorphous ice had been transformed to cubic phase. The temperature 0.57 revolution before the megaburst comes out to be 106°.30 K, lower by only 0°.07 K compared to the nominal scenario. The duration of the megaburst in the two scenarios is also virtually identical, differing by less than 0.01 percent. The only nontrivial difference is 3°.6 K in the final temperature, which accounts for the 5.36 percent of ice transformed by the time of the last aphelion, 0.57 revolution before the megaburst. Indeed, for amorphous-to-cubic transformation complete to 100 − 5.36 = 94.64 percent, the nominal scenario yields a temperature of 186°.12 K, within 0°.05 K of the final value in Table 2. It is recalled (Sec. 6) that the temperatures in Table 2 require nontrivial corrections due to heat transport from the surface over the nearly 16 revolutions. This temperature rise is investigated in Sec. 9.2. In the meantime, the nominal scenario provides a satisfactory approximation.

The most critical test for the scenarios involving CO-laden water ice is their compliance with the condition (3) that the released CO gas supplies enough momentum to lift off the terrain layer. To estimate the rate of CO molecules impinging on a unit area of the layer's base, I adopt Schmitt *et al.*'s (1989) CO/H_2O abundance ratio of 11 percent, which offers a fairly conservative estimate; Salyk *et al.* (2007) determined that this relative abundance was 14 ± 4 percent in comet 17P from their near-infrared observations on 2007 October 29-30, some 6 days after the megaburst had begun. Adopting, as before, 5 km^2 for the layer's base area and 0.1 day for the event's duration, the total number of 7 × 10^{35} H_2O molecules in the comet's atmosphere at the time of peak outgassing (Paper 1) suggests that the layer's base area may have been impacted by up to 7 × 10^{35} × 0.11/5 km^2/0.1 day ≈ 1.8 × 10^{20} CO molecules cm^{-2} s^{-1} released during the megaburst, which is a sublimation rate of CO at a temperature of 47°.3 K. On the other hand, with a conservative value of 0.2 km/s for the velocity of escaping CO molecules, the liftoff of a 50-meter thick layer requires from condition (3) a minimum rate of 1.8 × 10^{19} CO molecules cm^{-2} s^{-1}, equal to a sublimation rate at 43°K and a factor of 10 lower than the peak estimated rate. For a higher, more realistic, velocity of superheated CO (Sec. 8), the required minimum rate would be still lower.

Table 2. Evolution of water ice temperature and crystallization rate over long periods of time.

Time before 2007 megaburst (revolutions[a])	Water ice temperature (K)	Fraction of ice in cubic phase (percent)
15.57	100.03	0.00
14.57	100.15	0.10
13.57	100.28	0.20
12.57	100.41	0.32
11.57	100.56	0.44
10.57	100.72	0.58
9.57	100.90	0.73
8.57	101.10	0.89
7.57	101.33	1.08
6.57	101.59	1.30
5.57	101.89	1.56
4.57	102.25	1.87
3.57	102.72	2.26
2.57	103.34	2.79
1.57	104.29	3.61
0.57	106.30	5.36
0.00	186.07	100.00

[a] Units of a mean orbital period about the Sun; comet 17P/Holmes averaged 7.18 years or 2623 days per revolution between 1892 and 2007; 0.57 revolution is time elapsed from the final aphelion before the megaburst.

◇ ◇ ◇

(text continued from page 105)

In summary, the *release of trapped carbon monoxide from water ice during its crystallization near 140°K generates a momentum that greatly exceeds the limit needed to lift off the terrain layer 50 meters thick.* Layers hundreds of meters thick could in fact be lifted off from the nucleus. The next step is an examination of major features of the crystallization process.

8. Possible Scenarios for Layer's Liftoff

With the critical test successfully passed, various scenarios are possible, depending on the partitioning of the energy of trapped CO molecules upon their release. On the one hand, one can argue that the megaburst was a product of the action of carbon monoxide alone, because its release proceeded so rapidly that there was no time to transfer any of the energy carried by CO to water ice. On the other hand, there may have been enough time for a *fraction* of this energy to be used for increasing the temperature of water ice in cubic phase.

The latter scenario is supported by the high H_2O outgassing rates for comet 17P/Holmes observed within days after the onset of the megaburst, unless much of the escaping mass of water was contained initially in icy grains (Sec. 10). On 2007 October 25-27, Combi *et al.* (2007) reported large amounts of atomic hydrogen, a dissociation product of water, in the comet's atmosphere and derived a water-production rate of $\sim$ 40 tons per second. Biver *et al.*'s (2008) estimate is even higher — a total outgassing rate of some 200 tons per second on 2007 October 25.9 UT. This number includes many gas species, but water vapor clearly dominated.[3] If no energy were transferred from released CO (and other trapped gases), the water ice temperature of $\sim$ 190°K (Figure 1) at the time the amorphous-to-cubic transformation was

[3] Much insight into the enormity of volatile losses suffered by comet 17P during the megaburst is provided by Biver *et al.* (2008). Even though they detected eleven molecular species, including hydroxyl (OH), their published production rate variations, starting with October 25.9 UT, refer to only five volatiles: carbon monoxide (CO), methanol (CH_3OH), hydrogen sulfide (H_2S), hydrogen cyanide (HCN), and carbon monosulfide (CS). The production rates show nearly identical temporal variations, dropping off more steeply than exponentially. The five species can be divided into three groups: the highest production rates were found for CO and CH_3OH, lower rates for the rest, by a factor of 3 for H_2S and by a factor of 10 for CS and HCN. On October 25.9 UT, the total mass production rate for these species is estimated at about 20 tons per second, or 10 percent of Biver *et al.*'s (2008) estimate of the total on that date. Other species, but mainly water should account for the 90 percent of the total. Since the outgassing rate must have peaked very shortly after the event's onset, probably within a very small fraction of a day, the genuine peak production rates in the early hours UT on October 24 should have been about a factor of 10 higher — *i.e.*, a total of 2×10^9 g/s. Even if continuing for only 3 hours, the atmosphere would have contained 2×10^{13} g of gas, about 20 percent of the total estimated mass of dust in the halo and equivalent to 7×10^{35} molecules of water, in agreement with an estimate in Paper 1 and moderately higher than indicated by Schleicher's (2009) results.

completed would imply a water sublimation rate of 1.4×10^{17} molecules cm^{-2} s^{-1}. For an outgassing area of 5 km^2, this corresponds to a production rate of only 0.2 ton per second, too low by a factor of 200 to 1000 (or more) compared to the estimates based on observations. A likely interaction between water ice and carbon monoxide (and other gases) upon the release is corroborated by Bar-Nun and Laufer's (2003) laboratory experiments showing that the prominent spike of an escaping volatile gas was correlated with a less-conspicuous spike of water vapor.

To determine the amount of energy that the observations require to be transferred from released carbon monoxide to water ice, I calculate, for a 5 km^2 terrain layer, the water-sublimation rates per unit surface area that are equivalent to Combi *et al.*'s (2007) and Biver *et al.*'s (2008) production rates. The results are, respectively, 2.7×10^{19} and 13.5×10^{19} molecules cm^{-2} s^{-1}, with the corresponding water-ice temperatures of 227°K and 242°K. Since the water-ice temperature was 189?7 K at the end of the crystallization process when there was no contribution from CO (Sec. 7), the energy rates required by the two higher temperatures are, by integrating Eq. (5), 6.1×10^8 erg g^{-1} and 8.9×10^8 erg g^{-1}, respectively. If this energy is provided by the explosively released CO molecules, then not only the observed high water-production rates are explained, but the sublimating water ice alone supplies enough momentum to lift off the terrain layer, as the rates exceed, by a factor from > 2 to > 10, the minimum required sublimation rate of 1.2×10^{19} molecules cm^{-2} s^{-1} (Sec. 4).

The next test of the proposed mechanism is provided by the observed halo-expansion velocity of 0.50 km/s (Sec. 1 and Paper 1). It is necessary to show that a significant fraction of dust particles in the cloud, into which the layer collapses upon the liftoff, is accelerated to such a high terminal velocity. A *thermal* velocity of 0.2 km/s, which CO molecules acquire near 50°K and which was used intentionally as a conservative estimate (near the end of Sec. 7), would not suffice — and neither would a *thermal* velocity of water molecules, not even in a temperature range of 227°K to 242°K, given the inferred high dust-mass loading of the water flow (a dust-to-water mass ratio of ~ 5).

The solution to this problem is provided by the fact that velocities of superheated carbon-monoxide molecules escaping from water ice at temperatures around 140°K should have been much higher than the thermal velocity at 50°K. I am unaware of any laboratory data on velocities of CO molecules released from water ice during the phase change, but a notion that they are a source of considerable energy is based not only on the explosive nature of the phenomena observed in the laboratory, but also on a significant difference between the activation energies in the expressions for the crystallization rate of pure water ice in Eq. (4) on the one hand and CO-laden water ice in Eq. (19) on the other hand. This difference, which provides information on an energy stored in superheated carbon monoxide trapped in water ice, is equal to $(5940 - 5370) \cdot k_B = 7.87 \times 10^{-14}$ erg per H_2O molecule or 2.63×10^9 erg per gram of water ice, where k_B is the Boltzmann constant. With water ice holding 11 percent of CO, whose molecules are nearly 1.6 times heavier than water, this energy is equivalent to 1.54×10^{10} erg per gram of CO. Should all this energy have become kinetic, the escape velocity of CO would be 1.75 km/s, which is in reality an upper limit.

Given the "runaway" temperature behavior just before the termination of the crystallization process, the release of CO should reasonably be approximated by an adiabatic explosion, for which the front of the escape velocity wave is strongly supersonic (Huebner 1976)

$$v_{\rm front} = \frac{2 v_{\rm sound}}{\Gamma - 1}, \tag{20}$$

where Γ is the specific-heat ratio for carbon monoxide, $v_{\rm sound}$ the speed of sound,

$$v_{\rm sound} = \sqrt{\frac{\Gamma k_B T}{m_{\rm CO}}}, \tag{21}$$

and $m_{\rm CO}$ the mass of a CO molecule. With $\Gamma = 1.4$, Eq. (20) gives a Mach number of 5 for carbon monoxide, and at 140°K the wave-front velocity is 1.2 km/s, or six times the thermal velocity of CO near 50°K.[4] The corresponding kinetic energy is ~ 47 percent of the total released energy estimated from the difference between the activation energy of pure and CO-laden water ice.

CO velocities in excess of 1 km/s are generally in a range that one would expect based on the observed expansion velocity of the dust halo, because due to a very high dust-mass loading of the CO flow, the dust-to-CO velocity ratio should not exceed $\sim \frac{1}{2}$ (see Figure 2 of Probstein 1969). Probstein's gas-dynamics model provides a solution that is applicable to submicron-sized dust particles injected into the halo of comet 17P/Holmes during the megaburst. For any such microscopic grains, up to, say, $s_0 \simeq 1$ micron in diameter, that practically "instantly" accommodate to the gas flow (having Probstein's similarity parameter $\beta \sim s_0/D \to 0$), Probstein's model offers a tight lower limit to the terminal velocity $(v_{\rm dust})_\gamma$, when the dust-to-CO mass-production-rate ratio γ is very high (estimated at $\gamma = 10^{14}/10^{12.55} \approx 30$ for the megaburst), namely

$$(v_{\rm dust})_\infty = \lim_{\gamma \to \infty} \left[\lim_{\beta \to 0} v_{\rm dust} \right] = \sqrt{2 C_{\rm dust} T}, \tag{22}$$

[4]Strongly supersonic velocities of parent molecules in emissions from comet 17P associated with the megaburst of 2007 are supported by Drahus *et al.*'s (2008a) observations at millimeter wavelengths. Monitoring the J(1-0) transition of HCN and the J(3-2) transition of CS between October 25 and 31, they found the line profiles to suggest a gas-expansion velocity of about 1 km/s, whereas their submillimeter observations of the J(3-2) transition of HCN one month later (Drahus *et al.* 2008b) indicated a lower gas-expansion velocity, probably near 0.5 km/s.

where $C_{\rm dust}$ is the specific heat of the dust and T is the relevant gas temperature. Equating $C_{\rm dust}$ with $C_{\rm layer}$ of the terrain layer (Sec. 9), $C_{\rm dust} \simeq 8 \times 10^6$ erg g^{-1} °K^{-1}, and taking $T \simeq 140$°K (at the peak of CO release; Figure 1), I find that $(v_{\rm dust})_\infty = 0.47$ km/s, in excellent agreement with the dust halo's observed expansion velocity.

In summary, both carbon monoxide and water (ice and vapor) from the putative reservoir contribute actively to the mechanism of lifting off, from the nucleus of comet 17P/Holmes, a $\sim$ 50-meter thick, rapidly collapsing terrain layer. Trapped in amorphous water ice, carbon monoxide is released during the phase transformation, a process that is exothermic and rapidly accelerating with time even in the absence of CO. At temperatures nearly 100°K higher than in its usual sublimation regime, trapped carbon monoxide is superheated, as illustrated by a significant activation-energy difference between the crystallization of pure and CO-laden water ice. As CO executes its supersonic, explosion-like escape, the temperature and sublimation rate of water ice increase strikingly due to the crystallization-driven exothermic reaction and, probably, also because some of the energy transferred from outpouring CO molecules.

Evidence based on observations of the megaburst of comet 17P suggests that carbon monoxide or water vapor were, on their own, capable of providing a momentum exceeding the minimum required for lifting off a terrain layer of the assumed properties (a base area of $\sim$ 5 km^2, a thickness of $\sim$ 50 meters, and a mass of $\sim 10^{14}$ g at a bulk density of 0.4 g cm^{-3}), given a mass of activated water ice of $\sim 2 \times 10^{13}$ g in the reservoir beneath the layer and a relative CO-to-H_2O mass ratio of 0.17. However, carbon monoxide was clearly the *primary momentum driver*, explaining the high dust-halo expansion velocity of 0.50 km/s, whereas energy transfer to water ice may account for the high water-production rates observed.

In terms of the overall energy involved, the exothermic reaction, assumed to set in when the temperature of the water-ice reservoir reached $\sim$ 106°K, provided some 2×10^{22} erg to increase the temperature to $\sim$ 190°K. Superheated carbon monoxide escaping during the phase transition is estimated to have contributed more than 5×10^{22} erg, of which probably 1.3 to 1.9 $\times 10^{22}$ erg could have been spent to raise the ice temperature to a general range of 230°K to 240°K and to sublimate ice at peak rates of up to $\sim 2 \times 10^8$ g/s, with about 2.6×10^{22} erg or more converted into the kinetic energy of CO. In Paper 1, the kinetic energy of the dust halo was estimated at 2.5×10^{22} erg, consistent with the above numbers.

9. Long-Term Heat Transfer Through Terrain Layer

The validity of the presented mechanism for lifting a terrain layer from the surface of comet 17P, applicable to the formation of major companions of nontidally split comets and to the super-massive explosions alike, is conditioned on a propitious regime of heat transport through the layer, with a constrained time scale necessary to reach the initial (aphelion) temperatute $T_{\rm init}$ of $\sim$ 106°K, as defined in Sec. 7 and Figure 1. This time scale should be short enough in order to accommodate the observed recurring events (Paper 2).

Comet 17P/Holmes has been prominently featured in this paper because it is the only comet for which the super-massive explosions, interpreted as products of a liftoff, or jettisoning, from the nucleus of collapsed terrain layers, have been observed on two different occasions. The first time in 1892-1893 as a pair of explosive episodes some 10 weeks apart and the second time as the megaburst of 2007, unrivaled in terms of the total mass of dust injected into the coma.

9.1. The Objective and Methodology of the Problem

The objective is to establish the thermophysical properties of a terrain layer, which are consistent with observations rather than to explore a particular model in detail. This is achievable with major simplifications in the general problem of heat transfer. In particular, since heat transfer is achieved both by conduction and by a flow of volatile species, especially water vapor, the two processes are lumped up into a single, effective coefficient of thermal conductivity, $K_{\rm eff}$, whose determination from the constraints listed below is the goal of this exercise. This *a posteriori* approach contrasts with the traditional *a priori* methodology for modeling heat transfer, whose drawback is the dependence on the choice of the coefficients of thermal conductivity for the dusty, icy, and vapor components in a comet's nucleus, the parametric values adopted by various authors often differing by orders of magnitude.

Specific to comet 17P/Holmes, two conditions from the results of Secs. 7 and 8 are as follows: (i) a critical aphelion temperature of 106°.3 K is to be reached at the base of the layer (at an areal location L_1 on the nucleus) to be jettisoned later during the same orbit; and (ii) the aphelion temperature of 106°.3 K is to be reached again, ν_0 revolutions later, at the base of another layer somewhere else on the nucleus (at an areal location L_2), *etc.* On the assumptions that (a) the interval of time $\nu_{\rm obs}$, which separates the 1892-1893 and 2007 super-massive explosions of comet 17P, represents a current mean recurrence time ν_0 for layer jettisoning, $\nu_0 = \nu_{\rm obs} = 16$ revolutions; and (b) the comet's entire surface is covered with such layers; one can, using the symbols of Sec. 4, define ν_0^*, a mean recurrence time for layers stacked on top of each other at any given areal location, by

$$\nu_0^* = \nu_0 \frac{\pi D^2}{A_{\rm layer}}. \tag{23}$$

This equation says that after all surface layers have been jettisoned from the comet, the process returns to location L_1: the layer originally stacked beneath the already removed layer is now, ν_0^* revolutions later, being jettisoned as well, *etc.* For an assumed average base area of a layer, $A_{\rm layer} \simeq 5$ km^2 (Sec. 2), on the nucleus of 17P — itself about 3.3 km in diameter (Lamy *et al.* 2000; Snodgrass *et al.* 2006) — I find that $\nu_0/\nu_0^* \simeq 0.146$ and that jettisoning of layers originally stacked in the interior of the nucleus on top of one another recurs, statistically, every $\nu_0^* \simeq 110$ revolutions. This means

that ν_0^* is equal to the mean "lifespan" of a layer on the surface of 17P and that the search for an effective coefficient of thermal conductivity $K_{\rm eff}$ that satisfies a jettisoning rate of one layer per 16 revolutions can for comet 17P be conducted as a search for $K_{\rm eff}$ that implies a mean lifespan of 110 revolutions for a layer on the surface, an equivalence that makes the approach to the problem more straightforward. Unless the physical conditions of the liftoff process change, ν_0^* is by definition time independent. On the other hand, from Eq. (23) it follows that, because the dimensions of the nucleus shrink episodically (as layers are removed), ν_0 increases with time.

The rest of this subsection deals with the problem of determining the rate of solar heat penetration into the nucleus that is consistent with the time scale provided by the known super-massive explosions experienced by comet 17P/Holmes in 1892-1893 and again in 2007. The solution requires the determination of the temperature distributions in the nucleus with time and depth beneath the surface, which are products of heat transfer through the nucleus. The process of heat transfer is described by a well-known partial differential equation, which in its simplified form is

$$C_{\rm layer}\rho_{\rm layer}\frac{\partial T}{\partial t} = K_{\rm eff}\nabla^2 T, \tag{24}$$

where $C_{\rm layer}$ is the layer's effective specific heat and $\rho_{\rm layer}$ its bulk density for which I use the value from Sec. 4. The specific heat for a dozen or so terrestrial analogues for comet refractory material, from ashes, coke, basalt rock, and graphite to silica, quartz, limestone, and sandstone are all known to have their specific heat between 7.1 and 9.2 $\times$ 10^6 erg g^{-1} °K^{-1}. The specific heat of water ice is in the same range at the temperatures between 89°K and 111°K. An adopted value of 8 $\times$ 10^6 erg g^{-1} °K^{-1} is an acceptable compromise. The values of $C_{\rm layer}$ and $\rho_{\rm layer}$ used in solutions to Eq. (24) are not very critical for two reasons: (i) it is only a thermal diffusivity κ,

$$\kappa = \frac{K_{\rm eff}}{C_{\rm layer}\rho_{\rm layer}} = \frac{1}{32}K_{\rm eff}10^{-5}{\rm cm}^2{\rm s}^{-1}, \tag{25}$$

that counts; and (ii) in spite of the uncertainties in $C_{\rm layer}$ and $\rho_{\rm layer}$, these quantities are known with higher accuracy than the coefficient of thermal conductivity.

The problem of heat transfer in the nucleus of comet 17P will be solved in one dimension, along the radial direction of a spherical coordinate system, in which case the partial differential equation (24) becomes

$$\frac{\partial T}{\partial t} = \kappa\left(\frac{\partial^2 T}{\partial z^2} + \frac{2}{z}\frac{\partial T}{\partial z}\right), \tag{26}$$

where z is a depth below the surface of the spherical nucleus. If Δz and Δt are constant steps in, respectively, depth z and time t, a recurrent formula that for any $i \geq 0$ gives $T(i+1, j)$, the temperature at time $(i+1)\ \Delta t$ and depth $j\Delta z$, in terms of $T(i, j-1)$, $T(i, j)$, and $T(i, j+1)$, the temperatures at time $i\Delta t$ and at depths $(j-1)\Delta z$, $j\Delta z$, and $(j+1)\Delta z$, is in the adopted coordinate system

$$T(i+1, j) = \zeta\left[\left(1 + \frac{1}{n-j}\right)T(i, j-1) - 2T(i, j) + \left(1 - \frac{1}{n-j}\right)T(i, j+1)\right] + T(i, j) \tag{27}$$

for $j = 1, 2, \ldots, n-1$, and

$$T(i+1, n) = T(i+1, n-1) \tag{28}$$

for the center of the nucleus, $n = \frac{1}{2}D/\Delta z$. This numerical integration scheme provides a procedure for determining the two-dimensional distribution of temperature $T(i, j)$ in the nucleus, with

$$\zeta = \frac{\kappa\Delta t}{(\Delta z)^2} \tag{29}$$

being a dimensionless parameter, i, j, and n being integers, and D being again the diameter of the nucleus. Because temperature variations generally decrease with increasing heliocentric distance, the practical solution to Eqs. (27) and (28) is substantially accelerated in Sec. 9.2 when time is replaced by true anomaly as an integration variable. Introducing a constant step in true anomaly, Δu, into the expression (29) for the coefficient ζ, I find

$$\zeta = \frac{\kappa[q(1+e)]^{\frac{3}{2}}\Delta u}{k(1+e\cos u)^2(\Delta z)^2}, \tag{30}$$

where k is the Gaussian gravitational constant, q and e are, respectively, the perihelion distance and eccentricity of 17P, and u is the true anomaly at time t. Expressing κ in units of cm^2/s, u in deg, z in cm, and q in AU, the constant $1/k$ = 0.8766 $\times$ 10^5.

The integration of Eq. (27) is carried out over all depths of stacked layers, from the surface to the center of the nucleus and over a number of revolutions about the sun, ν^*, from aphelion to aphelion. The first revolution, $\nu^* = 1$, spans over the values of i for which $0 \leq i \leq m$, where $m = 360°/\Delta u$; the second spans over i for which $m \leq i \leq 2m$, *etc.*, and the ν^*-th revolution over $\mu - m \leq i \leq \mu$, where $\mu = m\nu^*$ and ν^*, m, and μ are all integers. The integration is stopped when $\nu^* = \nu_0^*$, the layer's lifespan on the surface, as dictated by the initial temperature $T_{\rm init}$ (Sec. 9.2).

The choice of steps Δz and Δu is subject to two constraints. For Δz, one is given by requiring that $\mathrm{mod}(\frac{1}{2}D, \Delta z) = 0$, the other by a condition that the step be short enough that for any $0 \le i \le \mu - 1$ the difference $|T(i, j+1) - T(i, j)| < \epsilon_z$ be small enough that the error accumulated by integration over the nucleus does not propagate to reach unacceptably large values. Similarly, for Δu, one constraint is given by requiring that $\mathrm{mod}(360°, \Delta u) = 0$, the other by a condition that the step be short enough that for any $1 \le j \le n$ the difference $|T(i+1, j) - T(i, j)| < \epsilon_u$ be small enough that the error accumulated by integration over ν_0^* revolutions does not propagate to reach unacceptably large values.

In practice, to make sure that ϵ_z and ϵ_u have been chosen properly, the entire integration is run twice, with the originally selected steps Δz and Δu and with steps $\frac{1}{2}\Delta z$ and $\frac{1}{2}\Delta u$. If both runs give, after ν_0^* revolutions, temperature distributions that are identical to a prescribed precision, for example to 0°.01 K, the steps Δz and Δu are acceptable. If the prescribed precision is not achieved, temperature distributions with steps $\frac{1}{2}\Delta z$ and $\frac{1}{2}\Delta u$ are replaced with steps $\frac{1}{4}\Delta z$ and $\frac{1}{4}\Delta u$, *etc.* One can also test separately the steps in depth z and true anomaly u, keeping the other provisionally constant.

For a given scenario, determined by a set of chosen physical and orbital parameters (which therefore become "known" quantities), the resulting temperature distribution also depends on the choice of an initial condition and a boundary condition. The initial condition is a prescribed variation of the temperature $T(0, j)$ with depth $z = j\Delta z$, at a starting aphelion, $u = -180°$. I choose this condition in the form

$$T(0, j) = \Theta + \frac{\Phi}{1 + \Lambda(z/z_0)^\theta}, \qquad 0 \le j \le n, \tag{31}$$

where Θ, Φ, Λ, and θ are the parameters that must be determined from four constraints (one of which is a boundary condition) that are discussed below, and z_0 is an arbitrary normalizing depth. Unlike Eq. (27), Eq. (31) applies to the surface ($j = 0$) as well, and the initial (aphelion) surface temperature is $T_{\mathrm{surf}}^{(0)} = T(0, 0) = \Theta + \Phi$.

The boundary condition states that the sun's energy incident on an element of the comet's surface at a given time t is spent in part on thermal re-radiation, and in part on conduction of heat into the interior. Since the layer is assumed to be inert (Sec. 6), the boundary condition has no sublimation sink and can be written as follows:

$$(1 - A)\psi \frac{Q_0}{r^2} = \varepsilon\sigma T_{\mathrm{surf}}^4 - K_{\mathrm{eff}} \left(\frac{\partial T}{\partial z} \right)_{\mathrm{surf}}, \tag{32}$$

where σ is the Stefan-Boltzmann constant, A and ε are, respectively, the Bond albedo and the effective emissivity of the surface, ψ is an incidence-mode factor, Q_0 is the solar constant, r and T_{surf} are the comet's heliocentric distance and the equilibrium surface temperature at time t, and K_{eff} is the coefficient of thermal conductivity from Eqs. (24) and (25). In the initial condition, $T_{\mathrm{surf}} = T_{\mathrm{surf}}^{(0)}$. The second term on the right-hand side has a minus sign because the depth is reckoned from the surface inward: the energy sink due to heat conduction into the interior is positive when the gradient $(\partial T/\partial z)_{\mathrm{surf}}$ is negative.

The other three conditions are represented by prescribing initial (aphelion) equilibrium temperatures T_1 and T_2 at two particular depths, determined by integers j_1 and j_2,

$$\begin{aligned} T_1 &= T(0, j_1) \qquad \text{for} \quad z_1 = j_1 \Delta z, \\ T_2 &= T(0, j_2) \qquad \text{for} \quad z_2 = j_2 \Delta z, \end{aligned} \tag{33}$$

and by adjusting the coefficient Θ to fit a prescribed temperature in the center of the nucleus. The coefficient Φ is then simply

$$\Phi = T_{\mathrm{surf}}^{(0)} - \Theta, \tag{34}$$

the exponent θ is derived from

$$\theta = \frac{\log\left[\left(T_{\mathrm{surf}}^{(0)} - T_2\right)(T_1 - \Theta)\right] - \log\left[\left(T_{\mathrm{surf}}^{(0)} - T_1\right)(T_2 - \Theta)\right]}{\log z_2 - \log z_1}, \tag{35}$$

and the factor Λ is found from either of two relations ($k = 1$ or 2)

$$\Lambda = \frac{T_{\mathrm{surf}}^{(0)} - T_k}{T_k - \Theta} \left(\frac{z_0}{z_k} \right)^\theta. \tag{36}$$

The set of Eqs. (32) and (34)-(36) is solved iteratively. Since the gradient $(\partial T/\partial z)_{\mathrm{surf}}$ is not known at the start of the iteration, it is taken to be zero, so that in the first approximation,

$$T_{\mathrm{surf}}^{(0)} = T(0, 0) = \left[\frac{(1 - A)\psi Q_0}{\varepsilon\sigma} \right]^{\frac{1}{4}} r_{\mathrm{aph}}^{-\frac{1}{2}}, \tag{37}$$

where $r_{\rm aph}$ is the aphelion distance in AU. This expression is employed to derive the first-approximation values of Φ, θ, and Λ from, respectively, Eqs. (34), (35), and (36). A new value of the gradient $(\partial T/\partial z)_{\rm surf}$ is then calculated from

$$\left(\frac{\partial T}{\partial z}\right)_{\rm surf} = \frac{T(0,1)-T(0,0)}{\Delta z} = -\Phi\Lambda\frac{(\Delta z)^{\theta-1}}{1+\Lambda(\Delta z/z_0)^{\theta}} \tag{38}$$

and inserted into Eq. (32) to compute an improved value of the surface temperature $T^{(0)}_{\rm surf}$. The steps starting with Eq. (34) are repeated until the convergence is achieved and the final values of $T^{(0)}_{\rm surf}$ and the parameters from Eq. (31) are found.

The choice of the temperatures T_1 and T_2 in Eq. (33) and the parameter Θ in Eq. (31), is constrained by an assumption that the nucleus of comet 17P had been heated up to temperatures not lower than 60°K prior to the megaburst. Thus, the processes that amorphous ice (pure or gas-laden) is subjected to at extremely low temperatures ($\ll$ 60°K) become irrelevant. For example, in Schmitt *et al.*'s (1989) setup, with samples of CO-laden water ice deposited under vacuum conditions at $\sim$ 10°K, CO molecules were observed to escape copiously between 25°K and $\sim$ 50°K. Bar-Nun *et al.* (1985) reported this phenomenon (for ice enriched by several volatiles including CO) to occur at temperatures 30°K to 55°K, explaining it by evaporation of the gas frozen on, rather than trapped in, the ice. Simultaneously, pure amorphous ice undergoes a transition from its high-density to low-density phase between 38°K and 68°K (Jenniskens and Blake 1994, 1996). Another process that starts in the same temperature range but continues to higher temperatures is annealing of amorphous ice (Laufer *et al.* 1987; Jenniskens and Blake 1994), when some trapped molecules get expelled by a temperature-dependent "settling" down of ambient water ice molecules. Annealing in CO-laden amorphous ice is apparent in Schmitt *et al.*'s (1989) experiments as a very gradual decrease in the CO-to-H_2O abundance ratio in a temperature range of 50°K to 130°K. While annealing near the surface of a newly arriving comet may drive its activity at large heliocentric distances (Meech *et al.* 2009), the effect is relatively small at the boundary of the putative ice reservoir tens of meters beneath the surface.

I now turn to the boundary condition at true anomalies for which $1 \le i \le n-1$. The temperature $T(i,1)$ is determined by $T(i-1,0)$, $T(i-1,1)$, and $T(i-1,2)$ via Eq. (27), while the equilibrium surface temperature $T_{\rm surf} = T(i,0)$ follows from a rewritten Eq. (32), which has become a quartic equation

$$\varepsilon\sigma\Delta z T^4_{\rm surf} + K_{\rm eff}T_{\rm surf} - \Omega = 0, \tag{39}$$

where

$$\Omega = (1-A)\psi\Delta z Q_0 r^{-2} + K_{\rm eff}T(i,1). \tag{40}$$

The quartic equation is readily solved by an iterative technique, such as Newton's method or the *regula falsi* method.

Since the examined heat-transfer problem is one-dimensional, the incidence-mode parameter ψ in the boundary condition describes, for a given location on the nuclear surface, the character of variations in the incident flux of the sun's radiation during each revolution. In the following, I consider three different insolation regimes:

(a) In a *standard scenario*, sometimes referred to as an isothermal case, the incident flux is assumed to vary in such a way that, on the average, it can be approximated, at any point of the orbit, by a constant ratio of the cross-sectional area of the spherical nucleus to its total surface area:

$$\psi = \frac{1}{4}. \tag{41}$$

The incident flux integrated over one revolution is

$$\Xi = \int_{(P)} \frac{\psi Q_0}{r^2}dt = \frac{1}{2}\pi S_0, \tag{42}$$

where P is the orbital period,

$$S_0 = \frac{Q_0}{k\sqrt{q(1+e)}}, \tag{43}$$

and other quantities are as in Eqs. (30) and (32).

(b) In a *perihelion scenario*, the spin axis is assumed to be situated in the orbital plane (obliquity of 90°) and the temperature is derived at the location of a rotation pole that points toward the sun at perihelion (the pole is at the subsolar point at perihelion). In this case,

$$\begin{aligned} \psi &= \cos u \qquad \text{for} \quad -90^\circ \le u \le +90^\circ, \\ &= 0 \qquad\quad \text{for} \quad -180^\circ \le u < -90^\circ \text{ and } +90^\circ < u \le +180^\circ. \end{aligned} \tag{44}$$

The integrated flux is in this case

$$\Xi = S_0 \int_{-\frac{1}{2}\pi}^{\frac{1}{2}\pi} \cos u du = 2S_0, \tag{45}$$

or 1.27 times greater than in the standard scenario. The term $(\partial T/\partial z)_{\rm surf}$ in the boundary condition (32) becomes an energy source rather than a sink, and the temperature near the surface increases with depth at times for which $\psi = 0$. Because of the higher value of Ξ, one may expect that heat transport into the nuclear interior proceeds more rapidly than in the standard scenario and that therefore ν_0 and ν_0^* should be a little smaller. The calculations show that this is not always the case.

(c) In an *offset scenario*, the obliquity is again 90°, but the chosen location is a rotation pole that is at the subsolar point at a position in the orbit characterized by true anomaly $u_{\rm sub}$, constrained by $-180° \le u_{\rm sub} \le +180°$ and $u_{\rm sub} \ne 0°$. In this case

$$\begin{aligned} \psi &= \cos(u - u_{\rm sub}) \qquad \text{for} \qquad -90° \le u - u_{\rm sub} \le +90°, \\ &= 0 \qquad\qquad\quad \text{for} \qquad -180° \le u - u_{\rm sub} < -90° \text{ and } +90° < u - u_{\rm sub} \le +180°. \end{aligned} \tag{46}$$

The value of Ξ is equal to that in the perihelion scenario, but the asymmetry of the incident-flux distribution should affect the rate of heating of the interface between the base of the layer and the outer boundary of the ice reservoir. The offset scenario examined in the following has $u_{\rm sub}$ corresponding to a heliocentric distance 2.44 AU at the 2007 megaburst.

◇ ◇ ◇

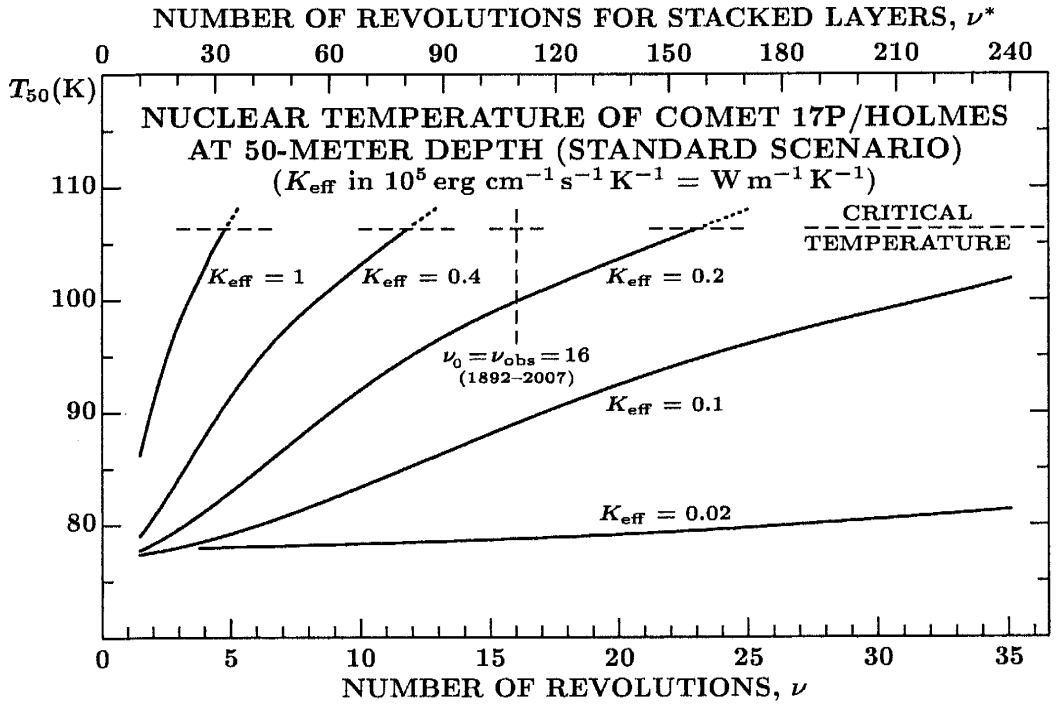

Figure 2. The temperature 50 meters beneath the surface of the nucleus of comet 17P, T_{50}, is plotted as a function of the number of completed revolutions, ν (lower axis), and a number of revolutions for stacked layers, ν^* (upper axis), for several values of the coefficient of thermal conductivity, $K_{\rm eff}$, in the standard scenario. The critical temperature of 106°.3 K and the 16 revolutions (separating the 1892-1893 and 2007 explosions) are depicted, intersecting near $K_{\rm eff} = 0.3 \times 10^5$ erg cm^{-1} s^{-1} $°K^{-1}$. Very similar plots can be constructed for the perihelion and offset scenarios.

◇ ◇ ◇

9.2. Results: Heat-Penetration Rate and Thermal Conductivity

The perihelion distance and orbital eccentricity, with which the computations are carried out, have been derived from the averaged values of perihelion and aphelion distances of the sets in Table 1 of Paper 2 for the 17 returns of comet 17P between 1892 and 2007. Because of the Jovian perturbations, the perihelion distance between 1913 and 1964 exceeded significantly those in 1892 and 2007, and this is reflected in the adopted mean values:

$$\langle q \rangle = 2.235\text{AU}, \qquad \langle e \rangle = 0.3978. \tag{47}$$

With these values, the offset scenario to be examined is described by $u_{\rm sub} = +45°$.

For a range of $0.01 < K_{\rm eff} < 2$ units of 10^5 erg cm^{-1} s^{-1} K^{-1} (called hereafter "K-units"),[5] the diffusivity κ has

[5] The CGS unit of 10^5 erg cm^{-1} s^{-1} $°K^{-1}$ = 1 W m^{-1} $°K^{-1}$, a unit that is often used in the literature.

been calculated from Eq. (25), and a temperature distribution derived from Eq. (27), using the initial and boundary conditions (with $A = 0.03$ and $\varepsilon = 1$) from Eqs. (31) and (32). The integration steps have been verified by the temperature distribution's convergence: $\Delta z = 25$ cm has always been acceptable, while Δu is thermal-conductivity dependent, decreasing from 0°.25 for the lowest values of $K_{\rm eff}$ to 0°.05 for the highest.

The integration has always begun at aphelion. In the initial condition, the temperature in the center of the nucleus has invariably been taken as 60°K and one of the two temperature control points in Eqs. (33) as 68°K at a depth of 50 meters, while the other, referred to a depth of 1 or 2 meters, has been assumed to range from 80°K to 120°K. Combined with the boundary condition, the values of the parameters Θ, Φ, Λ, and θ from Eq. (31) were determined together with the initial surface temperature. For example, for $K_{\rm eff} = 0.4$ **K**-unit the starting temperature of 120°K at a depth of 1 meter yields, with the other constraints, $\Theta = 59°.96$ K, $\Phi = 60°.98$ K, $\Lambda = 0.5480$ for $z_0 = 10$ meters, and $\theta = 1.54475$. The initial aphelion surface temperature has come out to be 120°.94 K.

The result of the integration — the mean lifespan of terrain layers on the surface, ν_0^*, when the aphelion temperature at a 50-meter depth reaches 106°.3 K — is a function of the effective thermal conductivity $K_{\rm eff}$ that measures a heat-penetration rate needed to reach the point of runaway crystallization (Figure 1 and Sec. 7) and therefore the time of jettisoning.

If desired, the integration may continue with the next layer. For this purpose, I save — as an input for the next run — the entire aphelion-temperature matrix, described by λ:

$$|| \, T(\lambda, 0), T(\lambda, 1), T(\lambda, 2), ..., T(\lambda, n-1), T(\lambda, n) \, ||, \tag{48}$$

in which n is the number of steps in depth [as in Eqs. (27)-(28)] and $\lambda = m\nu_0^*$, with m being again the number of true-anomaly steps per orbit ($m \geq 1440$ for $\Delta u \leq 0°.25$). The next run begins by replacing λ with zero.

◇ ◇ ◇

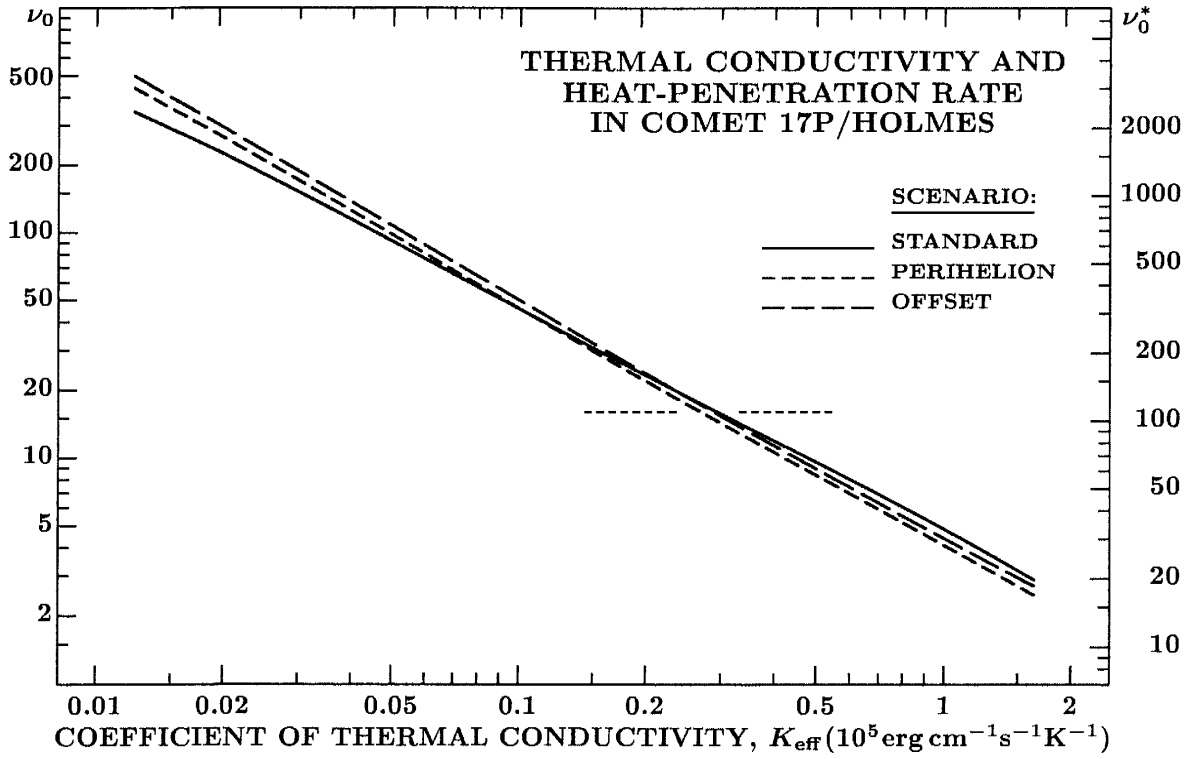

Figure 3. The number of completed revolutions, ν_0 (and ν_0^*), needed for the temperature to reach 106°.3 K at a 50-meter depth, is plotted as a function of the effective coefficient of thermal conductivity, $K_{\rm eff}$, in the three insolation regimes introduced in Sec. 9.1. The values of $K_{\rm eff}$ that correspond to $\nu_0 = \nu_{\rm obs} = 16$ revolutions (or $\nu_0^* = 110$ revolutions), marked by a dotted horizontal line, are between 0.26 and 0.30 × 10^5 erg cm^{-1} s^{-1} °K^{-1}.

◇ ◇ ◇

Experience with applying the integration scheme shows that it can also be used to completely eliminate the effects of an arbitrary initial condition on the temperature distribution; two iterations of the integration run are necessary, with a correspondingly decreasing size of the nucleus (due to layer jettisoning) incorporated in the successive input files. In the standard scenario with $K_{\rm eff} = 0.4$ **K**-unit, for example, the first cycle with the arbitrarily chosen initial condition has shown that a temperature of 106°.3 K was reached at a 50-meter depth for a mean lifespan of the layer on the surface

of $\nu_0^* = 93$ revolutions ($\nu_0 \simeq 14$ revolutions), with an aphelion surface temperature of 130°2 K. After the first iteration, $\nu_0^* = 82$ revolutions, while the second and higher iterations have converged to $\nu_0^* = 81$ revolutions ($\nu_0 \simeq 12$ revolutions). The aphelion surface temperature has remained at 130°2 K.

[text continued on page 115]

◇ ◇ ◇

Table 3. Temperature distribution in the nucleus of comet 17P/Holmes along its orbit about the Sun as a function of depth beneath the surface for three insolation regimes and with the aphelion temperature reaching 106.3 K at depth of 50 meters.

Orbital position[a] $(u, t-t_\pi, r)$	Assumed insolation regime[b]	Temperature (K) at depth (m) beneath the surface						
		0	1	2	5	10	50	100
−180°	S	129.3	140.3	147.8	152.4	145.2	106.3	76.5
−1306	P	103.0	125.3	142.2	158.6	147.6	106.3	76.4
5.188	O	108.4	133.4	150.4	157.7	143.9	106.3	77.5
−150°	S	130.4	137.3	143.8	151.1	145.3	106.3	76.5
−868	P	99.7	119.5	135.3	155.4	148.0	106.4	76.4
4.766	O	103.4	124.6	140.5	155.3	144.4	106.3	77.5
−90°	S	152.7	145.3	144.0	148.2	145.4	106.3	76.6
−331	P	95.0	111.5	125.6	149.0	148.4	106.4	76.4
3.124	O	97.2	114.0	128.0	148.8	145.2	106.3	77.5
−45°	S	173.0	158.9	151.4	147.4	145.3	106.4	76.6
−137	P	222.4	165.6	141.7	144.9	148.2	106.4	76.5
2.438	O	94.1	109.0	121.8	144.2	145.2	106.4	77.5
−20°	S	179.9	165.6	156.3	147.8	145.2	106.4	76.6
−58	P	250.7	195.2	161.9	144.6	147.9	106.4	76.5
2.274	O	197.6	141.7	127.3	141.8	145.1	106.4	77.5
0°	S	182.1	169.4	159.8	148.4	145.1	106.4	76.6
0	P	258.1	210.6	176.1	146.0	147.7	106.4	76.5
2.235	O	233.1	174.3	144.8	140.5	144.9	106.4	77.5
+20°	S	181.3	171.5	162.5	149.3	145.0	106.4	76.6
+58	P	252.9	218.3	186.9	148.6	147.4	106.4	76.5
2.274	O	248.4	196.2	162.2	140.8	144.6	106.4	77.5
+45°	S	176.2	171.2	164.4	150.6	144.9	106.4	76.6
+137	P	229.1	216.2	194.0	152.7	147.0	106.5	76.5
2.438	O	247.4	210.3	178.6	143.5	144.2	106.4	77.5
+90°	S	159.0	163.7	162.8	152.6	144.8	106.4	76.6
+331	P	132.9	177.5	185.1	159.7	146.7	106.5	76.5
3.124	O	204.0	203.1	188.7	151.3	143.6	106.4	77.6
+150°	S	134.9	146.9	153.2	153.3	145.0	106.5	76.7
+868	P	107.5	133.6	151.7	161.1	147.2	106.5	76.5
4.766	O	117.0	149.1	165.2	158.1	143.6	106.5	77.6
+180°	S	129.3	140.3	146.8	152.5	145.2	106.5	76.7
+1306	P	103.0	125.3	142.2	158.6	147.7	106.5	76.5
5.188	O	108.4	133.4	150.4	157.7	144.0	106.5	77.6

[a] True anomaly u, time from perihelion $t-t_\pi$ (days), and heliocentric distance r (AU) in an orbit determined by a perihelion distance of 2.235 AU and eccentricity of 0.3978. The corresponding mean osculating orbital period, 2612 days, differs slightly from the average perihelion-to-perihelion period between 1892 and 2007, and by nearly 100 days from the 2007 osculation orbital period (Sec. 7).

[b] Sunlight incidence mode scenario: S = standard, P = perihelion, O = offset; the respective coefficients of thermal conductivity, K_{eff}, are 0.292, 0.267, and 0.286 unit of 10^5 erg cm^{-1} s^{-1} K^{-1}.

The temperature at a depth of 50 meters, T_{50}, is for several values of $K_{\rm eff}$ shown in Figure 2 as a function of the number of completed revolutions, ν, and the number of revolutions for stacked layers, ν^*, in the standard scenario. Two most important effects to notice are (i) the best fit to $\nu = \nu_0 = \nu_{\rm obs} = 16$ revolutions, achieved by a temperature curve for $K_{\rm eff} \approx 0.3$ **K**-unit and (ii) a tendency of the temperature curves to level off with increasing ν (or ν^*).

The number of completed revolutions, needed for the temperature to reach 106°.3 K at 50 meters beneath the surface of the nucleus, is, as a function of the thermal-conductivity coefficient $K_{\rm eff}$, plotted in Figure 3 for each of the three insolation regimes introduced in Sec. 9.1. The figure shows that the relationship is nearly independent of the insolation regime and that for $\nu_0 = 16$ revolutions (or $\nu_0^* = 110$ revolutions) the value of $K_{\rm eff}$ is between 0.26 and 0.30 **K**-unit: 0.292 **K**-unit for the standard scenario, 0.267 **K**-unit for the perihelion scenario, and 0.286 **K**-unit for the offset scenario. The number of revolutions follows closely a $K_{\rm eff}^{-1}$ law, the actual mean values of the exponent being −0.98 for the standard scenario, −1.06 for the perihelion scenario, and −1.07 for the offset scenario.

With the results shown to be independent of the choice of the initial and boundary conditions, Figures 2 and 3 display the primary products of the heat-transfer calculations. A highly abridged extract of the generated time- and depth-dependent temperature distribution obtained in digital form is presented in Table 3. For each boundary condition, the tabulated temperatures represent examples of two-dimensional sets of data containing 6600 elements in depth and up to 7200 elements in true anomaly for each orbit about the sun, or a total of up to some 5 billion elements in integrations over ~ 110 revolutions.

◇ ◇ ◇

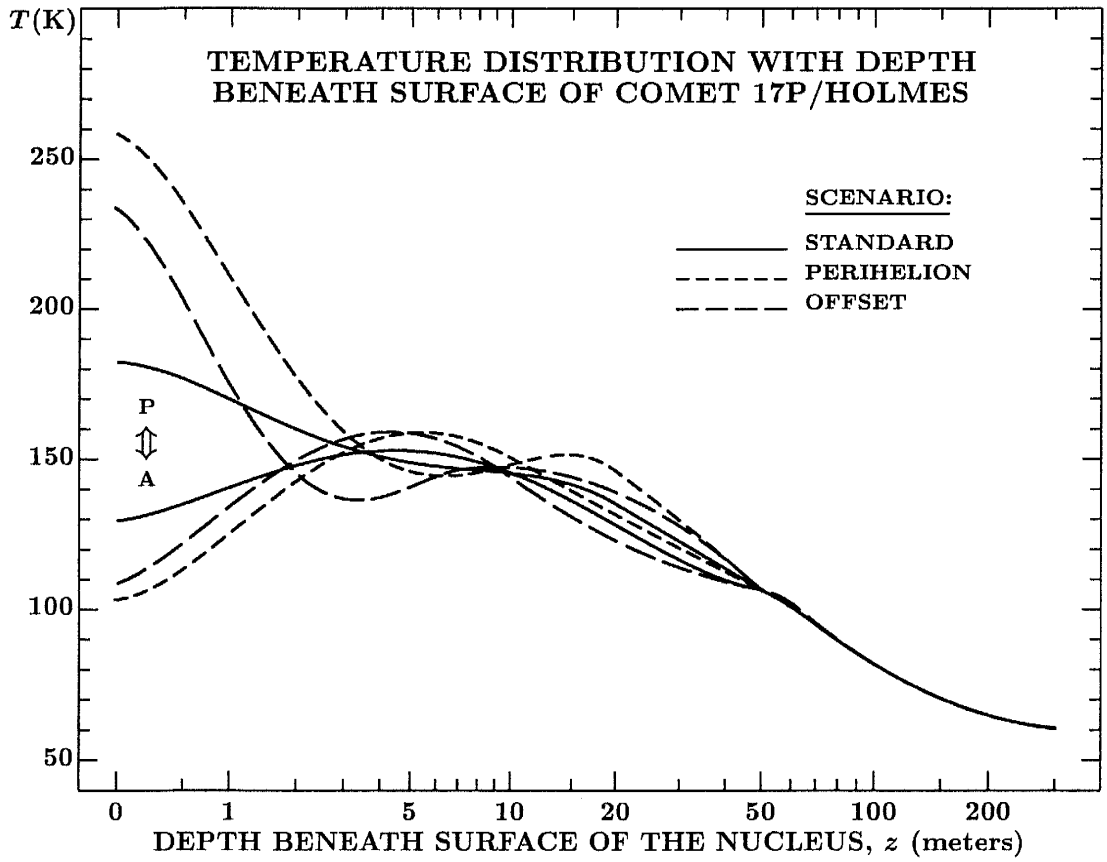

Figure 4. Temperature distribution with the depth beneath the surface of comet 17P when the temperature at a depth of 50 meters reaches 106°.3 K. The three insolation regimes are compared at the aphelion point (A), when the surface temperature is always below 150° K, and at the following perihelion point (P), when it is always above 150° K. Major differences, apparent among the three scenarios only at relatively shallow depths, include (i) the perihelion-to-aphelion surface and near-surface temperature amplitude, which is the least for the standard scenario and the largest for the perihelion scenario; and (ii) the near-surface temperature gradients, which are always positive (the temperature increasing with the depth) at aphelion but always negative at the following perihelion. The temperature at the center of the nucleus has stayed very near 60° K, within a small fraction of 1° K. The depth is plotted as $\log(1+z)$, *approaching a linear scale at* $z \ll 1$ *meter but a logarithmic scale at* $z \gg 1$ *meter.*

◇ ◇ ◇

Next I address, one by one, the implications of the temperature distribution and its relation to the CO-laden water-ice crystallization process (Sec. 7), the liftoff of a layer (Sec. 8), and the recurrence time of the super-massive explosions

(Sec. 9.1). I also compare the present conclusions on a heat-penetration rate and thermal conductivity of comet 17P with the results reported by other researchers in the literature.

Some of the most important features of the heat-transport process in the interior of the nucleus of 17P/Holmes during the orbit in which the temperature has reached 106°.3 K at a depth of 50 meters are exhibited in Figure 4. The temperature distribution for each of the three insolation regimes is plotted against the depth beneath the surface at the aphelion and following perihelion points of the orbit. The thermal flow from the surface into the interior, which is so prominently displayed at perihelion, is reversed at aphelion, showing that the surface becomes a thermal sink. The effect in the perihelion-to-aphelion surface-temperature amplitude between the standard scenario on the one hand and the perihelion and offset scenarios on the other hand is understood as a product of more extreme incident solar-flux variations characterizing the two latter insolation regimes. The oscillations in the subsurface temperature distribution at perihelion — including the secondary maxima and minima at the depths between ~ 3 and ~ 15 meters on the curves for the perihelion and offset scenarios — are driven by thermal lags.

◇ ◇ ◇

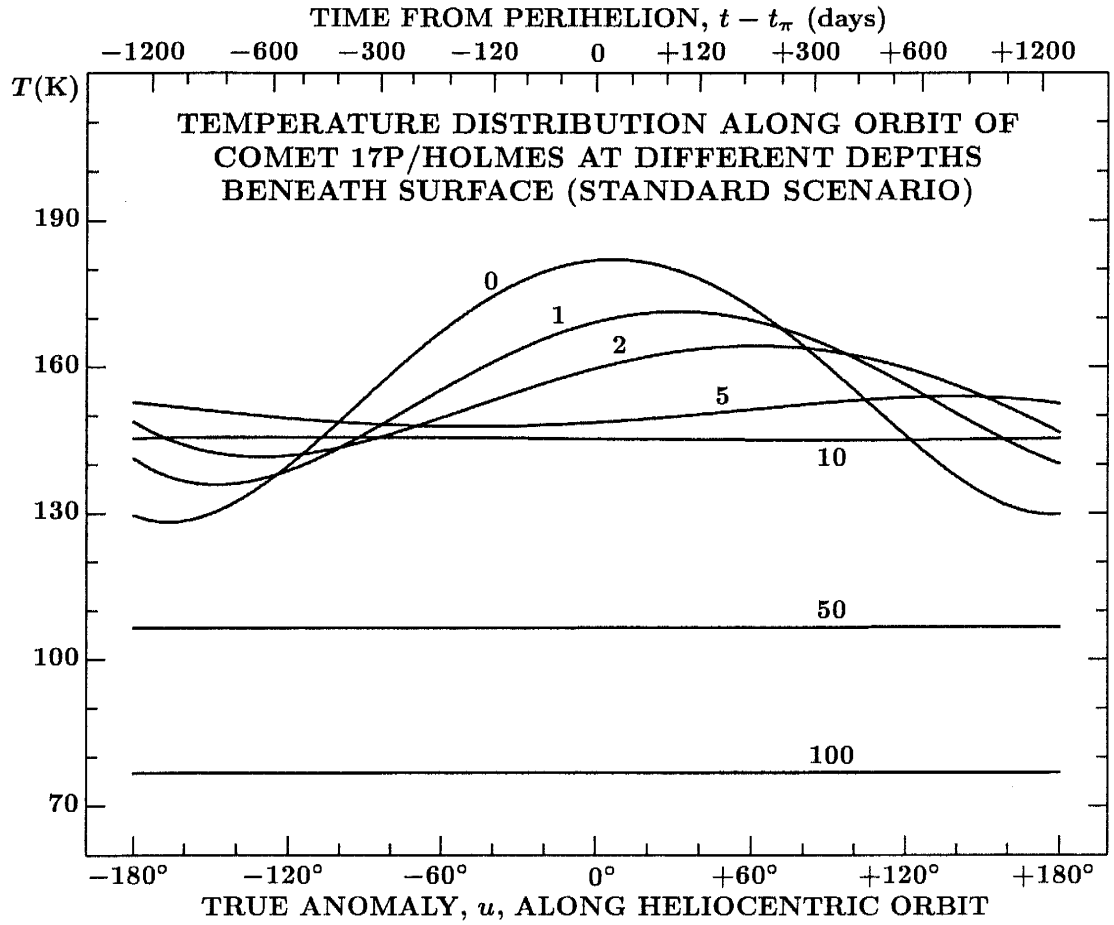

Figure 5. Surface and subsurface temperature distributions along the orbit of comet 17P when the temperature at a depth of 50 meters reaches 106°.3 K. The curves, each identified by the depth in meters, refer to the standard scenario, the other two scenarios exhibiting similar variations but with larger amplitudes and with steep temperature changes at and near the surface at the times of local sunrise and sunset. All curves in the figure show asymmetries relative to perihelion. The peak temperature is reached about 2 weeks after perihelion at the surface, but some 3 months, more than $\frac{1}{2}$ year, and more than 2 years at the depths of, respectively, 1, 2, and 5 meters. At 10 meters, the shift is nearly 90 percent of the orbital period and the amplitude less than 1° K. At still greater depths, the temperature continues to increase with time with no interruption. At 50 meters, the rate is 0°.15 K per revolution. The other scenarios show very similar temperature variations at depths greater than 10 meters.

◇ ◇ ◇

The most conspicuous effects are apparent in the orbital (temporal) variations of the temperature distribution, when examined as a function of depth. Displayed in Figure 5 for the standard scenario during the orbit in which the temperature reaches 106°.3 K at a 50-meter depth, the curves show that even though the amplitude of the temperature variations

steadily decreases with depth, the subsurface distribution exhibits an enormous and progressively increasing bias toward higher post-perihelion temperatures. Whereas the surface temperature reveals, as expected, a signature of the insolation regime (incidence-mode parameter ψ), the peak temperatures beneath the surface lag behind perihelion so profoundly that the rapidly cooling surface cannot keep up with the interior at depths as large as 10 meters or more at heliocentric distances greater than about 4 AU after perihelion. Compared to the standard scenario, this thermal inversion (with the interior warmer than the surface) is pronounced even more strongly for the perihelion and offset scenarios, when the surface (at the chosen location) receives no energy input from the sun over long periods of time. At depths of less than 50 meters, the temperature variations reach a *state of continuous rise throughout the orbit about the sun* regardless of the insolation regime. At a 50-meter depth, Table 3 shows that the mean rate of temperature increase becomes about 0°.15 K per revolution, which is consistent with the long-term trend against ν^* that is apparent from Figure 2 for the standard scenario near $K_{\rm eff} \simeq 0.3$ **K**-unit.

Comparison of this systematic, heat-transport-driven temperature rise with the results of Sec. 7, especially Table 2, reveals the existence of two parallel thermal processes at a nominal 50-meter depth, where the presented model assumes that the interface between the terrain layer and the ice reservoir is located. Both processes increase the temperature with time, but their thermophysical properties are different: (i) the water-ice crystallization accelerates the rate of increase with time in the temperature of the ice reservoir, causing its progressively steeper rise, while (ii) the rate of increase in the temperature of the layer's base, due to heat transport, slows down with time. The model suggests that until about 12 revolutions before the megaburst, the heat-transport effect dominates, then the crystallization effect takes over. Because, in reality, the ice reservoir is mixed with the refractory material of the layer over a range of depths (Sec. 6), the temperature of the interface region cannot be determined with high accuracy. However, the time scale for layer jettisoning must be shorter for a given thermal conductivity $K_{\rm eff}$, or $K_{\rm eff}$ must be lower for a prescribed number of revolutions ν^*, compared to the results in Figures 2-3 and Table 3. In an extreme case, when the two modeled rates of temperature increase in the interface region are summed up as if each applied to the whole mass, one finds that the critical temperature to be reached by the interface at aphelion 15 revolutions before the explosion is $\sim$ 97°.5 K, with the crystallization process accounting for about 6°.3 K (Table 2) and the heat-transport process for additional $\sim$ 2°.5 K, relative to the nominal critical temperature of 106°.3 K. To fit the recurrence time of 110 revolutions, the resulting effective coefficient of thermal conductivity for the standard scenario must be decreased to

$$(K_{\rm eff})_{\rm final} \simeq 0.20 \ \ {\rm Wm^{-1}K^{-1}}, \tag{49}$$

and similarly for the other two insolation regimes.

The continuous, parallel action of the two processes, crystallization and heat transport, has another major implication for the resulting super-massive explosions. The nominal case considered in Sec. 7 referred to the megaburst of 2007, which began 172 days after perihelion (Paper 1; Sekanina 2009a), but the results can be generalized. Because of a correlation between the onset time of the super-massive explosion and the temperature at the layer's base at the time of the previous aphelion passage (Figure 2), this aphelion temperature can serve as a "gauge" of the onset time of the event. A change in the temperature at a rate of 0°.15 K per revolution implies a change of 110 days in the onset time, a higher temperature corresponding to an earlier onset time and *vice versa*. The onset times of the 1892-1893 and 2007 events, ranging from about 140 to some 220 days after perihelion (Paper 1 and Sekanina 2009a), are thus readily accommodated within the interval of 110 days and their post-perihelion timing is explained.

From the presentation of this theory, it is apparent that the recurrence time between two consective super-massive explosions of comet 17P — or any other comet for that matter — cannot by any stretch of circumstances be equated with a strict periodicity. The recurrence time depends not only on the thickness of the layer, but also on its thermophysical properties, structure, and other factors that determine the time needed for heat to penetrate it and reach the interface with the ice reservoir. To that extent, of course, the interval of 16 revolutions between the two super-massive explosions of 17P has no major statistical significance. However, the introduction of this constraint is important in that it provides an additional boundary condition for a particular, yet self-consistent and physically meaningful, solution.

9.3. Thermal Conductivity and Thermal Inertia: Comparisons

The history of investigation of thermal conductivity of cometary nuclei documents the controversial nature of the results by different authors and illustrates the problems encountered. The purpose of this section is to find out how the effective thermal conductivity, established in Sec. 9.2 for heat transport through terrain layers of comet 17P, compares with the published determinations based on independent data, methods, and/or models.

The efforts over the past 30 years (too numerous to comment on each of them) followed a number of avenues but can essentially be divided into two categories that have focused, respectively, on (i) amorphous water ice, by applying mostly laboratory techniques; and (ii) the nuclei of comets themselves, by estimating the thermal inertia $\Im$ at their surface. Defined in terms of the thermal conductivity $K_{\rm eff}$, the specific heat $C_{\rm eff}$, and the bulk density $\rho_{\rm eff}$, the thermal inertia is

$$\Im = (K_{\rm eff} C_{\rm eff} \rho_{\rm eff})^{\frac{1}{2}}. \tag{50}$$

Using $K_{\rm eff}$ from Eq. (49) and equating $C_{\rm eff}$ with $C_{\rm layer}$ and $\rho_{\rm eff}$ with $\rho_{\rm layer}$ from Eqs. (24) and (25), one finds $\Im \simeq 250$ units of 10^3 erg cm^{-2} s$^{-\frac{1}{2}}$ K^{-1} (called hereafter "$\Im$-units").[6] Amorphous ice does not contribute significantly to the effective thermal conductivity of terrain layers, which consist mostly of inert refractory material. Nevertheless, work on

[6] The CGS unit of 10^3 erg cm^{-2} s$^{\frac{1}{2}}$ °K^{-1} = 1 J m^{-2} s$^{-\frac{1}{2}}$ °K^{-1} = 1 W m^{-2} s$^{\frac{1}{2}}$ °K^{-1}, often used in the literature.

amorphous ice is an integral part of the progress in the published research on the thermophysical properties of comets and it is included here in a brief review of the results of these efforts.

Klinger (1980) appears to have been the first to examine implications of the thermal conductivity of amorphous water ice, $K_{\rm ice}$, on comets. He calculated $K_{\rm ice}$ from the thermal diffusivity $\kappa_{\rm ice}$, which in turn was derived from the velocity of sound in ice and the mean free path of photons. The constants he used gave $\kappa_{\rm ice} \simeq 0.003$ cm^2/s and $K_{\rm ice} \simeq 0.2$ **K**-unit near 80°K and 0.3 **K**-unit near 120°K, remarkably close to my result for $K_{\rm eff}$ in Eq. (49). Independently, Smoluchowski (1981) used the same approach to obtain a higher value of thermal diffusivity, $\kappa_{\rm ice} \simeq 0.01$ cm^2/s, and to emphasize the importance of porosity and a comet's rotation state.

Before the end of the 1980s, the first results were available from an ambitious German KOSI (Kometensimulation) Project of laboratory experiments aimed at small-scale mimicking a cometary nucleus in a DFVLR space simulator in Cologne, West Germany (Kochan *et al.* 1989). As part of this undertaking, Spohn and Benkhoff (1990) investigated the thermophysical properties of several KOSI samples, consisting of water ice with small admixtures of carbon dioxide ice and clay minerals. By modeling the measured thermal histories of the samples between 100°K and 200°K, they derived the thermal diffusivity κ between 0.0002 and 0.0007 cm^2/s, about one order of magnitude lower than Klinger's (1980) values. Spohn *et al.* (1989) also conducted parallel experiments, determining the thermal conductivity from temperature gradients in compact and porous water ice and an ice-and-dust mixture. For porous samples in a temperature range of 80°K to 170°K, they found $K_{\rm ice} = 0.25 \pm 0.05$ **K**-unit, independent of the temperature and composition and more than one order of magnitude lower than for their compact ice samples. This thermal conductivity closely agrees with Klinger's (1980) values and with my result for $K_{\rm eff}$ given by Eq. (49).

A startling result was published by Kouchi *et al.* (1992), who claimed that their laboratory examination of amorphous water ice samples led to a coefficient of thermal conductivity 4-5 orders of magnitude lower than Klinger's (1980) values. Kouchi *et al.* concluded that under these conditions internal heating of comets is negligible at depths greater than several tens of centimeters from the surface.

Kouchi *et al.*'s (1992) result has never been reproduced by another set of experiments. In particular, Bar-Nun and Laufer (2003), who conducted their own laboratory studies of large samples of argon-laden amorphous ice prepared at 80°K, obtained thermal conductivity coefficients in a range of 0.01-0.05 **K**-units, about one order of magnitude lower than Klinger's (1980) results. Bar-Nun *et al.* (2007) have argued that the thermal conductivity measured by Bar-Nun and Laufer (2003) is consistent with a tentative upper limit on the thermal inertia $\Im$ of the surface of comet 9P/Tempel, estimated by A'Hearn *et al.* (2005) at probably less than 100 $\Im$-units from thermal infrared data taken by the *Deep Impact* mission. Groussin *et al.* (2007) refined A'Hearn *et al.*'s (2005) result to $\Im < 50$ $\Im$-units, prompting Thomas *et al.* (2008) to remark that subsurface sublimation occurs at depths of no more than 2-3 cm and possibly less. These arguments compare very unfavorably with a total mass of 10^{14} g of dust lost during the 2007 megaburst of comet 17P (Paper 1), which, even when spread over the entire surface of the nucleus, would form a layer more than 7 meters thick.

The problem of thermal inertia appears, however, to be more complicated, as suggested by two independent investigations. From their study of 100 Jupiter family comets observed with the Spitzer Space Telescope, Fernandez *et al.* (2007a, 2007b) noted that not all of these objects have low thermal inertia, thus implying that there may exist categories of comets of different thermophysical properties. A new twist to the thermal-inertia controversy has emerged from a work by Davidsson *et al.* (2009), who analyzed near-infrared thermal emission spectra of features on the nucleus of comet 9P/Tempel, obtained by *Deep Impact*. From their careful thermophysical modeling of a temperature map, Davidsson *et al.* have concluded that the notion on the comet's extremely low thermal inertia is incorrect and due to neglect of effects of small-scale surface roughness. While they admit that in specific areas of the surface the thermal inertia may be as low as 40-380 $\Im$-units, it is much higher, 1000-3000 $\Im$-units, over wide swaths of the nucleus of 9P. Because $K_{\rm eff} \propto \Im^2$, the implied thermal conductivity is $\sim$ 3-30 **K**-units for high-inertia regions, but $\sim$ 0.005-0.5 **K**-unit for low-inertia areas. This suggests extreme variations in the thermal conductivity over the surface of 9P, reaching, astonishingly, nearly four orders of magnitude. It also appears that the inertia corresponding to the thermal conductivity coefficient in Eq. (49) is closer to the lower end of Davidsson *et al.*'s (2009) range.

Returning to 17P, heat transport through a terrain layer must be dominated by conduction. The effective $K_{\rm eff}$ is a function of the thermal properties of the layer's granular material in compact form, described by $K_{\rm comp}$, and the porosity p. Using Russel's (1935) simplified formula that neglects a minor effect of heat conduction through pores by radiation, one has

$$K_{\rm eff} = K_{\rm comp} \frac{1 - p^{\frac{2}{3}}}{1 - p^{\frac{2}{3}}(1 - p^{\frac{1}{3}})}, \tag{51}$$

where the porosity relates the bulk density $\rho_{\rm eff}$ to the mineralogical (intrinsic) density of compact material $\rho_{\rm comp}$,

$$p = 1 - \frac{\rho_{\rm eff}}{\rho_{\rm comp}}. \tag{52}$$

The refractory material is generally a mix of silicate and carbon-rich compounds described by $\rho_{\rm comp}$ and by $K_{\rm comp}$ that is also poorly known. In a recent study, Davidsson *et al.* (2007) adopted $K_{\rm comp} = 3.1$ **K**-units, the same value that Kossacki and Szutowicz (2008) assigned to the mineral core of dust particles in their models for subsurface sublimation of comet 9P/Tempel. This compares rather favorably with $K_{\rm comp}$ for some terrestrial analogues — *e.g.*, 1.3 **K**-units for fused silica, 1.6 **K**-units for amorphous carbon, 2.2 **K**-units for limestone, 2.8 **K**-units for granite, and 2.9 **K**-units for sandstone. For another potential analogue, ordinary chondrites of low porosity and an intrinsic density of 3.7 $\pm$ 0.1 g

cm^{-3}, Yomogida and Matsui (1983) measured an average thermal conductivity K_{comp} of 1.3 **K**-units at 100°K and 1.5 **K**-units at 150°K, with a range for individual samples from 0.3 to 3.8 **K**-units.

With $\rho_{comp} = 3.7$ g cm^{-3}, a bulk density $\rho_{eff} = 0.4$ g cm^{-3} requires a porosity as high as 0.89 from Eq. (52) and a thermal-conductivity coefficient $K_{comp} = 2.6$ **K**-units from Eq. (51), when K_{eff} is taken from Eq. (49). These findings are consistent with information on K_{comp} from the analogues, and so is the value of K_{eff} from Eq. (49) when compared with the effective thermal conductivity adopted for granular cometary material in recent studies of related nature. For example, modeling the evolution of the interior of a cometary nucleus, Prialnik (2000) adopted $K_{eff} = 0.6$ **K**-unit, while investigating the formation of a dust mantle on the surface, Rosenberg and Prialnik (2009) assumed $K_{eff} = 0.1$ **K**-unit.

The highest values of thermal inertia derived by Davidsson *et al.* (2009) are likely to imply a major contribution from gas-phase conductivity, possibly involving species more volatile than water. Smoluchowski (1982) estimated that at temperatures only moderately exceeding 200°K, the thermal conductivity due to a flow of CO_2 vapor through pores can easily reach $\sim$ 40 **K**-units equivalent to a thermal inertia of 3000 ℑ-units or more, consistent with the upper end of Davidsson *et al.*'s (2009) thermal-inertia range.

The thermal inertia in excess of 1000 ℑ-units is therefore realistic for regions of local activity at, or very close to, the surface of the nucleus, but not at great depths, at which the temperature is too low for gas-phase conductivity to dominate. On the other hand, the thermal conductivity on the order of 0.2 **K**-unit, suggested by this study, is consistent with that for a highly porous refractory medium, expected to fit a description of terrain layers that this investigation has focused on. Since the role of amorphous water ice is relatively unimportant in the process of heat transport through the layer, then even if the thermal conductivity of amorphous ice is one order of magnitude lower than that of granular material, this should have no major effect on the overall rate of heat penetration. To summarize, the current state of understanding of the thermophysical properties of the interior of cometary nuclei and the processes of heat transport offers no compelling evidence for invalidating the presented model for super-massive explosions of comet 17P/Holmes.

10. Discussion and Conclusions

In this paper, I present a comprehensive model for the mechanism of the super-massive explosions, which were experienced by comet 17P/Holmes in 1892-1893 and again in 2007 — and during each of which a mass of 10^{13} to 10^{14} grams of dust was injected with up to subkilometer-per-second velocities from the comet's nucleus into its atmosphere in the form of a uniformly expanding, sharply-bounded halo. The model applies equally to fragmentation events that give rise to companion nuclei of the split comets. In conformity with Belton *et al.*'s (2007) talps concept, the presented model is based on the assumption that the comet's nucleus consists of terrain layers, averaging 50 meters in thickness and 5 km^2 in base area. They cover the entire surface of the nucleus and are stacked on top of one another throughout the interior, except possibly near the center. The layers are separated and "glued" together by reservoirs of gas-laden amorphous water ice, whose existence is a critical prerequisite of the presented model. Used as a representative example of the trapped gas is carbon monoxide, which, next to water, is known to be one of the most abundant volatile substances in comets. On the other hand, neither of the two properties of the layers suggested by Belton *et al.* (2007) — their occurrence limited to the Jupiter family comets and primordial origin — are essential for the validity of the presented hypothesis.

As the thermal energy penetrates, over a number of revolutions about the sun, from the surface ever deeper into the interior, each layer — starting with the topmost — is gradually heated up, until the interface with the ice reservoir located beneath each layer reaches a temperature of about 100°K. Proceeding at a very slow pace at lower temperatures, the exothermic crystallization process — a transformation of the water ice in the reservoir from amorphous to cubic phase — is poised near 100°K to enter a stage of escalating growth of temperature with explosive consequences. A self-feeding mechanism sets in, as ever greater quantities of transformed ice release ever larger amounts of energy, causing the temperature to rise extremely rapidly (in less than 1 minute) from 150°K to about 190°K. In the course of this process, at temperatures of about 130°K to 150°K, superheated carbon monoxide (and/or other volatiles) trapped in amorphous ice is being suddenly released, further increasing the temperature and generating a momentum more than sufficient for lifting off a 50-meter thick layer from the nucleus.

A super-massive explosion differs from a fragmentation event in that the mass of the layer collapses upon the liftoff into a pile of predominantly microscopic debris that is promptly swept away by the gas flow into a halo and accelerated to subkilometer-per-second velocities. By contrast, in a major fragmentation event, a large fraction of the lifted mass survives nearly intact, as one piece or a few pieces, accelerated by the gas-generated momentum to low, usually submeter-per-second separation velocities. In either case, the total mass of released material is about the same, 10^{13} to 10^{14} grams, the difference between the two phenomena consisting apparently only in the jettisoned layer's degree of cohesion, or its mechanical strength (which is extremely low for super-massive explosions) and in the mass distribution of fragments (which has a steeper slope — *i.e.*, a greater preponderance of the smallest microscopic particles, for the explosions). Fragmentation events are nearly always accompanied by outbursts (events that are substantially less powerful than the super-massive explosions), containing the debris that broke off from the large fragment(s) during and/or just after the liftoff. All fragments, including the principal one, may subsequently be subjected to secondary and higher-order fragmentation, leading to ever greater number of ever less-massive subfragments and eventually resulting in the disintegration of some (or most) of the original fragments or, on relatively rare occasions, of the entire comet.

A critical attribute of the proposed theory of super-massive explosions is a characteristic timescale on which they recur and which measures a mean lifespan of layer exposure on the surface of a comet. This is where the recurrence time for the explosions of comet 17P/Holmes can be used to constrain the solution to heat transport through the layers. The observed recurrence time of 16 revolutions about the sun, or 115 years — the interval between the 1892-1893 explosive

episodes and the 2007 megaburst — implies the layers' mean lifespan of about 110 revolutions or about 800 years, given that the surface area of comet 17P is nearly seven times the base area of the considered terrain layer. The corresponding heat penetration rate requires that the effective thermal conductivity of a 50-meter thick layer be about 0.2 W m^{-1} $°K^{-1}$, within a range of values recently derived from the *Deep Impact* thermal data and also consistent with terrestrial and extraterrestrial analogues, if the porosity is near 0.9. The thermal conductivity of amorphous water ice may be nearly one order of magnitude lower, but water ice does not contribute significantly to heat transport through the mostly inert layers of refractory material. Since it is the diffusivity, rather than the thermal conductivity itself, that determines the temperature distribution in the nucleus, the coefficient $K_{\rm eff}$ is affected by the uncertainties in the product $C_{\rm eff}\rho_{\rm eff}$. If, for example, this product is known with an accuracy of ±50 percent, the derived thermal conductivity is $0.2^{+0.2}_{-0.1}$ W m^{-1} $°K^{-1}$.

The recurrence time of super-massive explosions must not be understood as a strict periodicity. Depending not only on a layer's thickness, but also its thermophysical properties and position on the nuclear surface, the insolation regime, the orbital dimensions, *etc.*, the recurrence time is likely to vary rather widely from layer to layer, implying an equally broad range of variations in the lifespan of layer exposure on the surface.

The presented model is supported by compelling evidence based on the observations of the 2007 megaburst of comet 17P, including the dust and water production rates, the carbon monoxide-to-water production rate ratio, and the total energy involved. An excellent agreement is found between the observed and predicted expansion velocity of the dust halo. The model also fits the timing of the comet's super-massive explosions within a span of ~ 110 days centered on a time about $\frac{1}{2}$ year post-perihelion, a result that covers the 2007 megaburst as well as both episodes of the 19th-century event. The water production rate may be explained either by accelerated H_2O sublimation due to transfer of some energy from CO or by a major fraction of H_2O being injected (by escaping CO) from the nucleus into the atmosphere in the form of icy grains that then continue to sublimate. From their laboratory experiments, Bar-Nun *et al.* (1985) reported massive ejection of ice grains at temperatures much lower and somewhat higher than, but not around, 135°K to 155°K, during the transformation of amorphous ice to cubic ice. On the other hand, Bar-Nun and Laufer (2003) observed a somewhat delayed (at ~ 160°K) and less conspicuous spike in the water production in their experiment's chamber (Sec. 7). Although either option — or the combination thereof — remains somewhat speculative, the one invoking heat transfer from the explosively released gas to ambient water molecules appears at present to be perhaps more promising. Neither option affects the model's validity.

In reality, the terrain layers will be not only of different thickness and areal extent, but each layer will be of uneven thickness from one place to another. The composition, bulk density, and thermal properties will also vary locally. Deviations from a uniform layer considered in this study will have implications for timing of layer jettisoning. In spite of the runaway nature of the crystallization process, it is unlikely that the entire layer will be lifted as one piece at exactly the same time. Instead, the momentum that drives the process may vary distinctly from location to location at any given time and the layer will begin to break up under stress and shear while still on the nucleus. As a result, the actual time of the liftoff will vary with the position. This nonuniformity should account for the discrepancy between the predicted duration of the megaburst, 0.1 day (Sec. 7), and the observed duration, 2.2 days (Sekanina 2009a).

This liftoff scenario suggests that the 2007 megaburst of comet 17P — or any other super-massive explosion for that matter — is likely to consist of a rapid sequence of related but separate short explosive episodes. The same conclusion was reached in Sekanina (2009a) based on the comet's light curve in the early phase of the megaburst. Also consistent with this scenario is an oval-shaped feature located asymmetrically inside the halo to the southwest of its center (the position of the comet's nucleus) and reported by many observers (*e.g.*, Moreno *et al.* 2008; Montalto *et al.* 2008; Lin *et al.* 2009; Watanabe *et al.* 2009) as an extension, a plum-like feature, a jet, a blob, or an isolated dust cloud. There is a general agreement that the center of this feature receded from the nuclear condensation at a rate of ~ 130 m/s in projection onto the plane of the sky, which suggests that this was not a sizable fragment.

Watanabe *et al.* (2009) listed the measured offsets of the feature's center from the nucleus on four consecutive days, 2007 October 25-28. I have used this data set as input to a computer code that determines the parameters of a standard fragmentation model (Sekanina 1982), tested in the past on several dozens of split comets. This model allows to solve for up to five parameters of the "companion" object — its separation time from the parent comet; its deceleration (due to a nongravitational force, a differential effect from anisotropic outgassing in the case of sizable fragments) relative to the principal nucleus; and components of the companion's separation velocity in the three cardinal directions defined by the comet's orbital plane and the right-handed coordinate system: radial (away from the sun), transverse, and normal (for details, see Sekanina 1982). Because of a strong correlation between the deceleration and the radial component of the separation velocity in Watanabe *et al.*'s data set, a two-step iterative, least-squares, differential-correction procedure has been used to derive the most-probable solution. Four parameters — the separation time, the deceleration, and the transverse and normal components of the separation velocity — have been calculated first from a number of converging computer runs, each for a different, constant radial component; and then its most probable value has been determined in the second step by searching for a minimum sum of squares of residuals of the four-parameter solutions. The results are presented in Table 4, which shows that the separation occurred just about halfway through the active phase of the megaburst, which extended from October 23.7 to 25.9 UT (Sekanina 2009a). This separation time in Table 4 agrees with both Colas and Lecacheux's (2007) estimate (October 24.8 UT or slightly earlier) and Watanabe *et al.*'s linearly extrapolated offsets (October 24.9 UT). Of particular interest is the deceleration, which is clearly due to solar-radiation pressure and comparable, within the relatively large errors of determination, to a peak value of essentially dielectric dust particles in the submicron-size range. The projected velocity of ~ 130 m/s appears to be a combined effect of the deceleration and the radial component of the separation velocity. The apparent elongation in the radial direction of this

cloud is due largely to intrinsic scatter in the grains' decelerations.

◇ ◇ ◇

Table 4. Fragmentation model for the center of a dust cloud located asymmetrically in the expanding halo of comet 17P/Holmes on the Subaru/COMICS images from 2007 October 25-28.

Separation of dust cloud from nucleus	
Separation date (UT)	2007 October 24.75 ± 0.29
Separation time after perihelion (days)	173.25
Heliocentric distance (AU) at separation	2.439
Distance from ecliptic (AU) at separation	0.796
Separation velocity (m s^{-1})	90 ± 38
Radial component	$+60 \pm 50$[a]
Transverse component	-50 ± 25
Normal component	-45 ± 21
Relative deceleration (units[b])	0.80 ± 0.47
Number of observations (offset pairs) used	4
Interval of time covered (days)	3
RMS residual (arcsec)	± 0.75
Individual residuals[c] (arcsec):	

Date 2007 (UT)	R.A.	Decl.	Date 2007 (UT)	R.A.	Decl.
October 25.5	0.0	+0.3	October 27.5	+1.1	+0.1
26.5	−0.8	−0.3	28.4	−0.4	0.0

[a] Estimated error.
[b] Units of Sun's gravitational acceleration, which is 0.593 cm s^{-2} at a distance of 1 AU.
[c] Observed minus computed offsets of the center of dust cloud from the nucleus in right ascension (including a factor cos Decl.) and declination.

◇ ◇ ◇

With the light-curve signature of an early minor explosion, mentioned above, the isolated dust cloud is a second piece of evidence showing that the megaburst of 2007 consisted of a number of separate episodes in rapid succession. The 19th-century event is not only a striking case demonstrating that the succession of episodes does not have to be at all rapid, but possibly yet another indication of two closely-timed explosions; Richter (1949) affirmed that the January 1893 episode itself consisted of two successive sub-episodes separated from one another by less than 1.7 days. Although uncertain, this possibility cannot be ruled out, especially not in the light of what is now known about the megaburst of 2007.

The base area of terrain layers may also vary substantially from case to case, with 5 km^2 being only a crudely estimated average in the talps model based on images of 9P/Tempel. Moreno *et al.* (2008) concluded that, during the 2007 megaburst of 17P, one of the comet's rotation poles pointed nearly exactly at the sun and that the halo (or the shell, as they call it) consisted of dust ejecta from the *entire sunlit hemisphere*. I doubt that this conclusion is accurate; nevertheless, if taken literally, the base area of the hemispherical layer would be 17 km^2 (rather than 5 km^2) and the mass of 10^{14} grams at an average bulk density of 0.4 g cm^{-3} requires that the layer's thickness be 15 meters. Since, in Moreno *et al.*'s rotationally stable configuration, it is only one hemisphere (rather than the whole surface) that serves as a source for super-massive explosions, the number of hemispherical layers is equal to the number of layers stacked on top of one another and $\nu_0 = \nu_0^* = 16$ revolutions for hemispherical layers. Integration of the equation of heat transfer suggests that a temperature of $\sim$ 106°K at a depth of 15 meters is reached after 16 revolutions when $K_{\rm eff} \simeq 0.18$ **K**-units and, after accounting for the temperature increase due to ice crystallization (Sec. 7), $K_{\rm eff}$ decreases to about 0.12 **K**-units, approximately a factor 1.7 lower than in the nominal case explored in detail in Sec. 9. The corresponding mean thermal inertia of such hemispherical layers is about 200 $\Im$-units.

Since carbon monoxide is unlikely to be the only gas trapped in amorphous ice, the total momentum, equal to the sum of the momenta contributed by the various species may even be higher than estimated for carbon monoxide alone, and jettisoning of terrain layers may still be easier. The generated momentum may also be affected by the possible formation and decomposition of clathrate hydrates, by radioactive decay in the interior of the nucleus, and by other possible processes, whose incorporation into a much more complex model is beyond the scope of this paper.

Amorphous ice in the reservoir is certain to be contaminated by dust. Although Spohn *et al.*'s (1989) experiments suggested that the presence of dust had no effect on the thermal conductivity of water ice, the general issue of thermophysical properties of contaminated amorphous ice needs to be revisited. Also examined in the presence of refractory particulates should be the ability of amorphous ice to trap volatile gases, the dependence of the crystallization rate on the temperature, and effects on the rate and energy of release of the trapped gases during the crystallization process.

Discussing several published interpretations for the origin of *smooth* terrains — included in Belton *et al.*'s (2007) talps hypothesis — Belton and Melosh (2009) have suggested that these features on the surface of comet 9P/Tempel could be recent formations, less than 700 orbits old and likely products of an ongoing process. The present model for super-massive explosions is independent of the origin of the individual layers and it is valid even when different layers have different histories and ages, as long as they have been separated from one another (but glued together) by reservoirs of gas-laden amorphous water ice, which could be much less massive than the terrain layers themselves. As for the low cosmic age, it is not the only explanation for the smooth, nearly craterless regions on the nucleus. The surface of layers incorporated into the comet during a relatively brief agglomeration phase would remain smooth regardless of their age, because they had been protected from cosmic bombardment by other layers stacked on top of them.

The central issue addressed in this study is the long-term evolution of periodic comets with layered morphology, including their aging, nontidal fragmentation, proclivity to super-massive explosions, and ultimate disintegration. Although intermittent dormant stages may be part of this evolutionary process, a terminal deactivation is not — with the possible exception of a small remnant of the original object as hypothesized in the talps model.

A different problem is presented by periodic comets that *have never been observed to fragment nontially or to undergo super-massive explosions*. If for at least some of them this is so because they *have never done so*, they represent a separate category of objects not characterized by layered morphology, possibly of another origin, and in any case not a subject of this study. Such comets may eventually become deactivated to a point of appearing indistinguishable from asteroids.

Acknowledgements

I thank D. W. E. Green for reading and commenting on the draft of this paper and for editorial work. This research was carried out at the Jet Propulsion Laboratory, California Institute of Technology, under contract with the National Aeronautics and Space Administration.

REFERENCES

A'Hearn, M. F.; M. J. S. Belton; W. A. Delamere; J. Kissel; K. Klaasen; L. A. McFadden; K. J. Meech; H. J. Melosh; P. H. Schultz; J. M. Sunshine; P. Thomas; J. Veverka; D. K. Yeomans; M. Baca; I. Busko; C. J. Crockett; S. M. Collins; M. Desnoyer; C. A. Eberhardy; C. M. Ernst; T. L. Farnham; L. Feaga; O. Groussin; D. Hampton; S. Ipatov; J.-Y. Li; D. Lindler; C. M. Lisse; N. Mastrodemos; W. Owen; J. E. Richardson; D. D. Wellnitz; and R. L. White (2005). "Deep Impact: Excavating Comet Tempel 1", *Science* **310**, 258-264.

Bar-Nun, A.; and D. Laufer (2003). "First Experimental Studies of Large Samples of Gas-Laden Amorphous 'Cometary' Ices", *Icarus* **161**, 157-163.

Bar-Nun, A.; G. Herman; D. Laufer; and M. L. Rappaport (1985). "Trapping and Release of Gases by Water Ice and Implications for Icy Bodies", *Icarus* **63**, 317-332.

Bar-Nun, A.; I. Pat-El; and D. Laufer (2007). "Comparison Between the Findings of Deep Impact and Our Experimental Results on Large Samples of Gas-Laden Amorphous Ice", *Icarus* **187**, 321-325.

Belton, M. J. S.; and J. Melosh (2009). "Fluidization and Multiphase Transport of Particulate Cometary Material As an Explanation of the Smooth Terrains and Repetitive Outbursts on 9P/Tempel 1", *Icarus* **200**, 280-291.

Belton, M. J. S.; P. Thomas; J. Veverka; P. Schultz; M. F. A'Hearn; L. Feaga; T. Farnham; O. Groussin; J.-Y. Li; C. Lisse; L. McFadden; J. Sunshine; K. J. Meech; W. A. Delamere; and J. Kissel (2007). "The Internal structure of Jupiter Family Cometary Nuclei from Deep Impact Observations: The 'Talps' or 'Layered Pile' Model", *Icarus* **187**, 332-344.

Biver, N.; D. Bockelée-Morvan; H. Wiesemeyer; J. Crovisier; R. Peng; D. Lis; T. Phillips; J. Boissier; P. Colom; E. Lellouch; and R. Moreno (2008). "Composition and Outburst Follow-Up Observations of Comet 17P/Holmes at the Nançay, IRAM and CSO Radio Observatories", in *Asteroids, Comets, Meteors 2008*, LPI Contr. 1405, Paper 8146. (Abstract.)

Bobrovnikoff, N. T. (1943). "The Periodic Comet 17P/Holmes (1892 III)", *Pop. Astron.* **51**, 542-551.

Chen, J.; and D. Jewitt (1994). "On the Rate at Which Comets Split", *Icarus* **108**, 265-271.

Colas, F.; and J. Lecacheux (2007). "Comet 17P/Holmes", *Cent. Bur. Electr. Tel.* 1111.

Combi, M. R.; J. T. T. Maekinen; J.-L. Bertaux; E. Quemerais; and S. Ferron (2007). "Comet 17P/Holmes", *IAU Circ.* 8905.

Davidsson, B. J. R.; P. J. Gutiérrez; and H. Rickman (2007). "Nucleus Properties of Comet 9P/Tempel 1 Estimated from Non-Gravitational Force Modeling", *Icarus* **187**, 306-320.

Davidsson, B. J. R.; P. J. Gutiérrez; and H. Rickman (2009). "Physical Properties of Morphological Units on Comet 9P/Tempel 1 Derived from Near-IR Deep Impact Spectra", *Icarus* **201**, 335-357.

Delsemme, A. H.; and D. C. Miller (1971). "Physico-Chemical Phenomena in Comets — III. The Continuum of Comet Burnham (1960 II)", *Planet. Space Sci.* **19**, 1229-1257.

Drahus, M.; L. Paganini; L. M. Ziurys; W. Peters; C. Jarchow; and P. Hartogh (2008a). "The Recent Mega-Outburst of Comet 17P/Holmes at Millimeter Wavelengths", in *Asteroids, Comets, Meteors 2008*, LPI Contr. 1405, Paper 8340.

Drahus, M.; L. Paganini; L. Ziurys; and W. Peters (2008b). "Comet 17P/Holmes", *Central Bureau Electronic Telegram* 1289.

Fernandez, Y. R.; M. S. Kelley; P. L. Lamy; I. Toth; O. Groussin; C. M. Lisse; M. F. A'Hearn; J. M. Bauer; H. Campins; A. Fitzsimmons; J. Licandro; S. C. Lowry; K. J. Meech; J. Pittichová; W. T. Reach; and H. A. Weaver (2007a). "Thermal Properties, Size Distribution, and Albedo Distribution of Jupiter-Family Comets", *Bull. Amer. Astron. Soc.* **39**, 497. (Abstract.)

Fernandez, Y. R.; M. S. Kelley; P. L. Lamy; W. T. Reach; I. Toth; O. Groussin; C. M. Lisse; M. F. A'Hearn; J. M. Bauer; H. Campins; A. Fitzsimmons; J. Licandro; S. C. Lowry; K. J. Meech; J. Pittichová; and H. A. Weaver (2007b). "Results from SEPPCoN, a Survey to Study the Physical Properties of the Nuclei and Dust of Jupiter-Family Comets", *Bull. Amer. Astron. Soc.* **39**, 827. (Abstract.)

Ghormley, J. A. (1968). "Enthalpy Changes and Heat-Capacity Changes in the Transformations from High-Surface-Area Amorphous Ice to Stable Hexagonal Ice", *J. Chem. Phys.* **48**, 503-508.

Groussin, O.; M. F. A'Hearn; J.-Y. Li; P. C. Thomas; J. M. Sunshine; C. M. Lisse; K. J. Meech; T. L. Farnham; L. M. Feaga; and W. A. Delamere (2007). "Surface Temperature of the Nucleus of Comet 9P/Tempel 1", *Icarus* **187**, 16-25.

Holmes, E. (1892). "Discovery of a New Comet in Andromeda", *Observatory* **15**, 441-443.

Huebner, W. F. (1976). "The Nucleus: Panel Discussion", in *The Study of Comets*, NASA SP-393, B. D. Donn, M. Mumma, W. Jackson, M. F. A'Hearn, and R. Harrington, eds., U.S. GPO, Washington, DC, pp. 597-605.

Jenniskens, P.; and D. F. Blake (1994). "Structural Transitions in Amorphous Water Ice and Astrophysical Implications", *Science* **265**, 753-756.

Jenniskens, P.; and D. F. Blake (1996). "Crystallization of Amorphous Water Ice in the Solar System", *Astrophys. J.* **473**, 1104-1113.

Klinger, J. (1980). "Influence of a Phase Transition of Ice on the Heat and Mass Balance of Comets", *Science* **209**, 271-272.

Kochan, H.; J. Benkhoff; A. Bischoff; H. Fechtig; B. Feuerbacher; E. Grün; F. Joo; J. Klinger; H. Kohl; D. Krankowsky; K. Roessler; W. Seboldt; K. Thiel; G. Schwehm; and U. Weishaupt (1989). "Laboratory Simulation of a Cometary Nucleus: Experimental Setup and First Results", Proc. *19th Lunar Planet. Sci. Conf.*, pp. 487-492.

Kossacki, K. J.; and S. Szutowicz (2008). "Comet 9P/Tempel 1: Sublimation Beneath the Dust Cover", *Icarus* **195**, 705-724.

Kouchi, A.; J. M. Greenberg; T. Yamamoto; and T. Mukai (1992). "Extremely Low Thermal Conductivity of Amorphous Ice — Relevance to Comet Evolution", *Astrophys. J.* **388**, L73-L76.

Lamy, P. L.; I. Toth; H. A. Weaver; C. Delahodde; L. Jorda; and M. F. A'Hearn (2000). "The Nucleus of 13 Short-Period Comets", *Bull. Amer. Astron. Soc.* **32**, 1061. (Abstract.)

Laufer, D.; E. Kochavi; and A. Bar-Nun (1987). "Structure and Dynamics of Amorphous Water Ice", *Phys. Rev. B* **36**, 9219-9227.

Lin, Z.-Y.; C.-S. Lin; W.-H. Ip; and L. M. Lara (2009). "The Outburst of Comet 17P/Holmes", *Astron. J.* **138**, 625-632.

Meech, K. J; J. Pittichová; A. Bar-Nun; G. Notesco; D. Laufer; O. R. Hainaut; S. C. Lowry; D. K. Yeomans; and M. Pitts (2009). "Activity of Comets at Large Heliocentric Distances Pre-Perihelion", *Icarus* **201**, 719-739.

Montalto, M.; A. Riffeser; U. Hopp; S. Wilke; and G. Carraro (2008). "The Comet 17P/Holmes 2007 Outburst: The Early Motion of the Outburst Material", *Astron. Astrophys.* **479**, L45-L49.

Moreno, F.; J. L. Ortiz; P. Santos-Sanz; N. Morales; M. J. Vidal-Nuñez; L. M. Lara; and P. J. Gutiérrez (2008). "A Model of the Early Evolution of the 2007 Outburst of Comet 17P/Holmes", *Astrophys. J.* **677**, L63-L66; **684**, L55 (erratum).

Palisa, J. (1893). "Ueber eine plötzliche Aenderung im Aussehen des Cometen 1892 III (Holmes)", *Astron. Nachr.* **132**, 15-16.

Patashnick, H.; G. Rupprecht; and D. W. Schuerman (1974). "Energy Source for Comet Outbursts", *Nature* **250**, 313-314.

Prialnik, D. (2000). "Modeling the Comet Nucleus Interior", *Earth, Moon, Planets* **89**, 27-52.

Prialnik, D.; J. Benkhoff; and M. Podolak (2004). "Modeling the Structure and Activity of Comet Nuclei", in *Comets II*, M. C. Festou, H. U. Keller, and H. A. Weaver, eds., Univ. Arizona, Tucson, pp. 359-387.

Probstein, R. F. (1969). "The Dusty Gas Dynamics of Comet Heads", in *Problems of Hydrodynamics and Continuum Mechanics*, F. Bisshopp *et al.*, eds., Soc. Industr. Appl. Math., Philadelphia, pp. 568-583.

Richardson, J. E.; H. J. Melosh; C. M. Lisse; and B. Carcich (2007). "A Ballistics Analysis of the Deep Impact Ejecta Plume: Determining Comet Tempel 1's Gravity, Mass, and Density", *Icarus* **190**, 357-390.

Richter, N. (1949). "Helligkeitsschwankungen der Kometen und Sonnentätigkeit. II. Statistik und Theorie abnormer Lichtausbrüche von Kometenkernen", *Astron. Nachr.* **277**, 12-30.

Rosenberg, E. D.; and D. Prialnik (2009). "Fully 3-Dimensional Calculations of Dust Mantle Formation for a Model of Comet 67P/Churyumov-Gerasimenko", *Icarus* **201**, 740-749.

Russel, H. W. (1935). "Principles of Heat Flow in Porous Insulators", *J. Amer. Ceram. Soc.* **18**, 1-5.

Salyk, C.; G. A. Blake; M. J. Mumma; B. P. Bonev; M. A. DiSanti; G. L. Villanueva; Y. Radeva; K. Magee-Sauer; and E. L. Gibb (2007). "Comet 17P/Holmes", *IAU Circ.* 8890.

Schleicher, D. G. (2009). "The Long-Term Decay in Production Rates Following the Extreme Outburst of Comet 17P/Holmes", *Astron. J.*. **138**, 1062-1071.

Schmitt, B.; S. Espinasse; R. J. A. Grim; J. M. Greenberg; and J. Klinger (1989). "Laboratory Studies of Cometary Ice Analogues", *Physics and Mechanics of Cometary Materials*, ESA SP-302, J. Hunt and T. D. Guyenne, eds., ESTEC, Noordwijk, Netherlands, pp. 65-69.

Sekanina, Z. (1982). "The Problem of Split Comets in Review", *Comets*, L. L. Wilkening, ed., Univ. Arizona, Tucson, pp. 251-287.

Sekanina, Z. (2008a). "Exploding Comet 17P/Holmes", *Int. Comet Quart.* **30**, 3-28. (Paper 1.)

Sekanina, Z. (2008b). "On a Forgotten 1836 Explosion from Halley's Comet, Reminiscent of 17P/Holmes' Outbursts", *Int. Comet Quart.* **30**, 63-74.

Sekanina, Z. (2009a). "Comet 17P/Holmes: A Megaburst Survivor", *Int. Comet Quart.* **31**, 5-23.

Sekanina, Z. (2009b). "Recurrence of Super-Massive Explosions and Orbital Evolution of Comet 17P/Holmes. I. Missed 1913-1957 Returns to the Sun", *Int. Comet Quart.* **31**, 45-65 (Paper 2).

Smoluchowski, R. (1981). "Amorphous Ice and the Behavior of Cometary Nuclei", *Astrophys. J.* **244**, L31-L34.

Smoluchowski, R. (1982). "Heat Transport in Porous Cometary Nuclei", *J. Geophys. Res.* **87**, A422-A424.

Snodgrass, C.; S. C. Lowry; and A. Fitzsimmons (2006). "Photometry of Cometary Nuclei: Rotation Rates, Colours and a Comparison With the Kuiper Belt Objects", *Mon. Not. Roy. Astron. Soc.* **373**, 1590-1602.

Spohn, T.; and J. Benkhoff (1990). "Thermal History Models for KOSI Sublimation Experiments", *Icarus* **87**, 358-371.

Spohn, T.; K. Seiferlin; and J. Benkhoff (1989). "Thermal Conductivities and Diffusivities of Porous Ice Samples at Low Pressures and Temperatures and Possible Modes of Heat Transfer in Near Surface Layers of Comets", *Physics and Mechanics of Cometary Materials*, ESA SP-302, J. Hunt and T. D. Guyenne, ESTEC, Noordwijk, Netherlands, pp. 77-81.

Stevenson, R.; J. Kleyna; and D. Jewitt (2009). "Transient Sub-Nuclei in Outbursting Comet 17P/Holmes", *Bull. Amer. Astron. Soc.* **41**, No. 3, Paper 23.02. (Abstract.)

Thomas, N.; C. Alexander; and H. U. Keller (2008). "Loss of the Surface Layers of Comet Nuclei", *Space Sci. Rev.* **138**, 165-177.

Thomas, P. C.; J. Veverka; M. J. S. Belton; A. Hidy; M. F. A'Hearn; T. L. Farnham; O. Groussin; J.-Y. Li; L. McFadden; J. Sunshine; D. Wellnitz; C. Lisse; P. Schultz; K. J. Meech; and W. A. Delamere (2007). "The Shape, Topography, and Geology of Tempel 1 from Deep Impact Observations", *Icarus* **187**, 4-15.

Watanabe, J.-I.; M. Honda; M. Ishiguro; T. Ootsubo; Y. Sarugaku; T. Kadono; I. Sakon; T. Fuse; N. Takato; and R. Furusho (2009). "Subaru/COMICS Mid-Infrared Observation of the Near-Nucleus Region of Comet 17P/Holmes at the Early Phase of an Outburst", *Publ. Astron. Soc. Japan* **61**, 679-685.

Yomogida, K.; and T. Matsui (1983). "Physical Properties of Ordinary Chondrites", *J. Geophys. Res.* **88**, 9513-9533.

Φ Φ Φ

Tabulation of Comet Observations

New CCD camera code: `FLM` = Finger Lakes Instrumentation (FLI) ML-8300-C [additional information available at website URL `http://www.flicamera.com/fli/microline.html`].

New CCD-chip code: `KA8` = Kodak KAF-8300-C.

Descriptive Information, to complement the Tabulated Data (all times UT):

See the July 2001 issue (page 98) for explanations of the abbreviations used in the descriptive information.

◇ *Comet 22P/Kopff* ⟹ 2009 July 16.94, 26.93, Aug. 16.92, 20.96, 24.93, 27.93, and 27.95: low alt. [SRB]. July 28.00: star of mag 16.0 located 1′ from central cond. [BRE03]. Aug. 3.36: obs. remotely from near Mayhill, NM, U.S.A. [SHU]. Aug. 14.67: possible long tail in p.a. 250° [TSU02]. Aug. 20.01: city lights; weather conditions excellent; comet hard to see, very diffuse; comet better seen w/ Swan-band filter (Lumicon comet filter) [PAR03]. Aug. 20.96: star of mag 14.8 located 0′.7 from the central cond. [SRB]. Aug. 22.59-22.60: LONEOS PKS 2345-167 sequence used for comp.-star mags [YOS02]. Aug. 23.93: star of mag 11.0 located 1′.0 from the central cond. [BRE03]. Aug. 24.93: star of mag 10.7 located 1′.1 from the central cond. [SRB]. Aug. 27.95: poor conditions [BRE03]. Aug. 31.31 and Sept. 1.36: obs. remotely from a site between Cloudcroft and Mayhill, NM, U.S.A. [SHU]. Sept. 11.91: obs. from Aralla (elev. 1360 m), León, Spain [GON05]. Sept. 20.74: bright and easy to see even in the low sky [YOS04]. Sept. 26.86: moonlight [BRE03]. Oct. 11.75: obs. remotely with 15-cm R at Pingelly, W. Australia [SHU].

◇ *Comet 29P/Schwassmann-Wachmann* ⟹ 2009 Sept. 23.19: "in evolution after a recent outburst"; zodiacal light; alt. 20° [GON05]. Oct. 26.21: zodiacal light; "the observed 3′ coma is a remnant of the previous outburst" [GON05].

◇ *Comet 43P/Wolf-Harrington* ⟹ 2009 Sept. 16.15: remotely from near Mayhill, NM, U.S.A. [CHE09].

◇ *Comet 47P/Ashbrook-Jackson* ⟹ 2009 Sept. 15.35: remotely from near Mayhill, NM, U.S.A. [CHE09].

◇ *Comet 64P/Swift-Gehrels* ⟹ 2009 Sept. 16.46: remotely from near Mayhill, NM, U.S.A. [CHE09].

◇ *Comet 65P/Gunn* ⟹ 2009 May 25.90: limiting mag ~ 15.0; nearby field stars checked via Palomar plates (Digitized Sky Survey) [LEH]. June 1.05 and July 24.91: (regarding the use of `TK` comparison-star mags for such a faint comet, see the reply by the observer under June 20.93, below, which he used as an example; note that Tycho-satellite-catalogue star magnitudes should generally not be used if possible for comets fainter than mag 11-11.5 — *Ed.*) [GON05]. June 20.93: "there were several Tycho-2 stars fainter than mag 12 (in the range 12.1-12.8) within a radius of 1°5 of the comet; in my experience, when preparing to observe comets in the 12- to 13-mag range, it is usually possible to find enough 12th-mag Tycho stars within a suitable radius; but, knowing that Tycho-2 stars below mag 11 are less reliable, I use TASS or Henden photometry in nearby fields, when possible (especially for fainter comets), taking into account the importance of the similar conditions in the in the sky background" [GON05]. June 22.19: remotely from near Mayhill, NM, U.S.A. [CHE09].